CIRJE-F-515

Estimating Stochastic Volatility Models Using Daily Returns and Realized Volatility Simultaneously

Makoto Takahashi
Graduate School of Economics, University of Tokyo

Yasuhiro Omori
University of Tokyo

Toshiaki Watanabe
Hitotsubashi University

September 2007 ; Revised in March 2008

CIRJE Discussion Papers can be downloaded without charge from:

http://www.e.u-tokyo.ac.jp/cirje/research/03research02dp.html

Discussion Papers are a series of manuscripts in their draft form. They are not intended for circulation or distribution except as indicated by the author. For that reason Discussion Papers may not be reproduced or distributed without the written consent of the author.

Estimating Stochastic Volatility Models Using Daily Returns and Realized Volatility Simultaneously

Makoto Takahashi

Graduate School of Economics, University of Tokyo, Tokyo 113-0033 Japan

Yasuhiro Omori

Faculty of Economics, University of Tokyo, Tokyo 113-0033 Japan

Toshiaki Watanabe *

Institute of Economic Research, Hitotsubashi University, Tokyo 186-8603 Japan

---

Abstract

Realized volatility, which is the sum of squared intraday returns over a certain interval such as a day, has recently attracted the attention of financial economists and econometricians as an accurate measure of the true volatility. In the real market, however, the presence of non-trading hours and market microstructure noise in transaction prices may cause the bias in the realized volatility. On the other hand, daily returns are less subject to the noise and therefore may provide additional information on the true volatility. From this point of view, modeling realized volatility and daily returns simultaneously based on well-known stochastic volatility model is proposed. Empirical studies using intraday data of Tokyo stock price index show that this model can estimate realized volatility biases and parameters simultaneously. Bayesian approach is taken and an efficient sampling algorithm is proposed to implement the Markov chain Monte Carlo method for our simultaneous model. The result of the model comparison between the simultaneous models using both naive and scaled realized volatilities indicates that the effect of non-trading hours is more essential than that of microstructure noise and that asymmetry is crucial in stochastic volatility models. Our Bayesian approach provides an estimate of the entire conditional predictive distribution of returns under consideration of the uncertainty in estimation of both biases and parameters. Hence common risk measures, such as value-at-risk and expected shortfall, can be easily estimated.

Key words: Asymmetry; Bias correction; Markov chain Monte Carlo; Multi-move sampler; Realized volatility; Stochastic volatility

---

1. Introduction

The financial return volatility, defined as the variance or the standard deviation of returns, plays a central role in the modern finance such as the option pricing and the evaluation of risk measures, e.g. value-at-risk (VaR) and expected shortfall. Realized volatility, which is the sum of squared intraday returns over a certain

* Corresponding author. Postal address: 2-1 Naka, Kunitachi City, Tokyo 186-8603 Japan, Phone: +81-42-580-8356, Fax: +81-42-580-8333, E-mail: watanabe@ier.hit-u.ac.jp.

interval such as a day, has recently attracted the attention of financial economists and econometricians as an accurate measure of the true volatility. The realized volatility, proposed by Andersen and Bollerslev (1998) and Barndorff-Nielsen and Shephard (2001) independently, would provide a consistent estimator of the latent volatility in the ideal market assumption.

In the real market, however, there are two problems in measuring daily realized volatility from high frequency return data. One problem is the presence of non-trading hours and the other is the presence of the market microstructure noise in transaction prices. Stock markets are open only for a part of a day. For example, Tokyo Stock Exchange (TSE) is open only for 4.5 hours a day. The realized volatility may underestimate the latent one-day volatility if we define the latent one-day volatility for day t as the volatility from the market closing time for day $t-1$ to that for day t as usual and calculate the realized volatility as the sum of squared intraday returns only when the market is open. To avoid this underestimation, Hansen and Lunde (2005) scale realized volatility using daily returns so that the mean of the realized volatility equals to the variance of the daily return.

On the other hand, the market microstructure noise has various sources, including discrete trading and bid-ask spread (see e.g., O'Hara (1995) and Hasbrouck (2007) for details). Due to the noise, the realized volatility can be a biased estimator of the latent volatility (see, e.g., McAleer and Medeiros (2006) for a review of the realized volatility and effects of the microstructure noise). As the time interval approaches to zero, the variance of the true price process independent of the market microstructure noise decreases and then the effect of the microstructure noise becomes more significant. This means that there is a trade-off between the variance and bias of the realized volatility. Considering this trade-off, Bandi and Russell (2005) derive a simple formula to produce the optimal time interval of intraday returns used for calculating the realized volatility. Zhang, Mykland, and Aït-Sahalia (2005) also propose the way to correct the bias by combining two realized volatilities calculated from returns with different frequencies.

While the intraday returns are heavily contaminated by the microstructure noise, the daily returns are less subject to the noise. Thus the daily returns may provide additional information on the latent volatility. From this perspective, this article models the daily returns and realized volatility simultaneously by extending stochastic volatility models with or without asymmetry between today's daily return and tomorrow's volatility.

We assume that the realized volatility includes the microstructure noise but still contains much information on the latent volatility. On the other hand, daily returns have less such noises but do not include the sufficient information on the latent volatility. Therefore, the model can correct the bias using all the available high frequency data. This feature is shared basically only by the two-scale estimator of Zhang et al. (2005) while all other volatility estimators are inefficiet in the sense that they discard a large amount of available data for correcting the bias. Additionally, the model can estimate the biases due to both the microstructure noise and non-trading hours simultaneously without an additional calculation to determine the optimal time interval using the formula of Bandi and Russell (2005), to compute several realized volatilities for calculating the two-scale estimator of Zhang et al. (2005), or to scale realized volatility as in Hansen and Lunde (2005). Further, modeling returns and realized volatility simultaneously has a certain advantage in that our model enables us to estimate the entire conditional predictive distribution of returns and hence common risk measures such as VaR and expected shortfall can be easily estimated.

However, it is difficult to evaluate the likelihood of our model analytically and hence to estimate the parameters in the model by the maximum likelihood method. Thus we develop a Bayesian method for estimating the parameters in our model using the Markov chain Monte Carlo (MCMC) technique. To make the estimation method efficient, we extend the block (multi-move) samplers proposed by Shephard and Pitt (1997) and Watanabe and Omori (2004) for symmetric stochastic volatility models and by Omori and Watanabe (2008) for asymmetric ones. The MCMC method also enables us to take account of the parameter uncertainty in predicting the distribution of returns.

We illustrate our model and estimation method by applying them to the daily data on returns and realized volatility of the Tokyo stock price index (TOPIX). We show that this model can estimate realized volatility biases and parameters simultaneously. Bayesian comparison between the simultaneous models using both two (naive and scaled) realized volatilities shows that the effect of non-trading hours is more essential than that of microstructure noise. Further, extending the simultaneous models with asymmetry improves the model fitting significantly.

The paper is organized as follows. In Section 2, we first describe how to compute the realized volatility and discuss two practical problems in such computations. Then we propose a simultaneous model and explain its estimation method using the MCMC technique. Section 3 applies our proposed model to the TOPIX data. Finally, Section 4 concludes.

2. Simultaneous Modeling of Stochastic Volatility and Realized Volatility

2.1. *Integrated Volatility, Realized Volatility, and Microstructure Noise*

We first consider a simple continuous time process,

$$\mathrm{d}p(s) = \sigma(s)\mathrm{d}w(s), \tag{1}$$

where $p(s)$ denotes the log-price of a financial asset at time s, and $\sigma^2(s)$ is the instantaneous or spot volatility which is assumed to have locally square integrable sample paths and stochastically independent of the standard Brownian motion $w(s)$. Then, the volatility for day t is defined as the integral of $\sigma^2(s)$ over the interval $(t, t+1)$ where a full twenty-four-hour day is represented by the time interval 1, i.e.,

$$IV_t = \int_t^{t+1} \sigma^2(s)ds,$$

which is called an integrated volatility.

Although the integrated volatility cannot be observed, we can estimate it using observable high frequency asset returns. Suppose that we have n intraday returns during each day t, $\{r_{t,i}\}_{i=1}^n$, then the precise volatility measure, called a realized volatility, is defined as the squared sum of them over day t, i.e.,

$$RV_t = \sum_{i=1}^{n} r_{t,i}^2. \tag{2}$$

In the ideal world, that is, if there were no market microstructure noise and the asset were always and continuously traded, the realized volatility would provide a consistent estimator of the integrated volatility, that is,

$$RV_t \to IV_t, \quad n \to \infty.$$

Equivalently, the discretization noise due to $\mathrm{d}w(s)$ in the realized volatility disappears as the time interval goes to zero.

In the real market, however, there are two problems in measuring the realized volatility. One problem is the presence of non-trading hours and the other is the existence of the market microstructure noise.

Stock markets are open only during a part of a day. For example, Tokyo Stock Exchange (TSE) is open only for four and a half hours a day. The realized volatility may underestimate the integrated volatility if we calculate the realized volatility as the sum of squared intraday returns only when the market is open. To avoid this underestimation, one may include returns on the non-trading hours (overnight and/or lunch time interval) but this can make the realized volatility noisy because such returns have much discretization noise. Thus, Hansen and Lunde (2005) propose scaling realized volatility for the market open period as

$$SRV_t = cRV_t, \quad c = \frac{\sum_{t=1}^T (R_t - \bar{R})^2}{\sum_{t=1}^T RV_t},$$

where R_t is the daily return, T is the daily sample size, and $\bar{R} = T^{-1}\sum_{t=1}^T R_t$. This ensures that the mean of the scaled realized volatility (SRV) is equal to the variance of daily returns.

On the other hand, to deal with the market microstructure noise, we denote the observed intraday log price as $p_{t,i}$ and suppose that the observed log price can be written as

$$p_{t,i} = p^*_{t,i} + \varepsilon_{t,i},$$

where $p^*_{t,i}$ is the true intraday log price and $\varepsilon_{t,i}$ is the microstructure noise. Then we can write the observed intraday return as the true intraday return $r^*_{t,i} = p^*_{t,i} - p^*_{t,i-1}$ plus the disturbance $\nu_{t,i} = \varepsilon_{t,i} - \varepsilon_{t,i-1}$, i.e.,

$$r_{t,i} = p_{t,i} - p_{t,i-1} = r^*_{t,i} + \nu_{t,i}. \tag{3}$$

Therefore, the realized volatility is given by

$$RV_t = \sum_{i=1}^{n} (r^*_{t,i})^2 + 2\sum_{i=1}^{n} r^*_{t,i}\nu_{t,i} + \sum_{i=1}^{n} \nu^2_{t,i}.$$

From this expression, we observe that the realized volatility can be a biased estimator of the integrated volatility. If the true log price $p^*_{t,i}$ follows the equation (1), the mean of $\sum_{i=1}^{n}(r^*_{t,i})^2$ converges in probability to the integrated volatility as the time interval approaches to zero (equivalently, n goes to infinity). On the other hand, the expected value of $\sum_{i=1}^{n}\nu^2_{t,i}$ increases. For example, if $\varepsilon_{t,i}$ has a constant variance σ^2_ε independent of the time interval and no autocorrelation, the expected value of $\sum_{i=1}^{n}\nu^2_{t,i}$ is equal to $2n\sigma^2_\varepsilon$. This means that the bias caused by the microstructure noise increases as the time interval approaches to zero. Considering this trade-off between the variance and the bias of the realized volatility, Bandi and Russell (2005) derive a simple formula to produce the optimal time interval.

Bandi and Russell (2005) also show that $RV_t \to \infty$ in the case that $\varepsilon_{t,i}$ has zero mean and is a covariance stationary stochastic process; the variance of $\nu_{t,i}$ is $O(1)$. Additionally, when the noise $\varepsilon_{t,i}$ is an independently and identically distributed random variable and is independent of the price process, Zhang et al. (2005) show that RV_t has a bias and a larger variance due to the noise. They also propose a way to correct the bias by combining two realized volatilities calculated from returns with different frequencies, which is called two-scaled realized volatility (TSRV).

To calculate TSRV, first the original return series, $\{r_{t,i}\}^n_{i=1}$, is partitioned into subsamples, $\{r_{t,i}\}^{(l)}$, $l = 1, \dots, L$, where $n/L \to \infty$ as $n \to \infty$. For example, for $\{r_{t,i}\}^{(1)}$ start at the first observation and take an observation every 5 minutes; for $\{r_{t,i}\}^{(2)}$, start at the second observation and take an observation every 5 minutes, etc. Calculating realized volatility for each subsample, which we denote $RV^{(l)}_t$, and averaging them give rise to the estimator

$$RV^{(\text{avg})}_t = \frac{1}{L}\sum_{l=1}^{L} RV^{(l)}_t.$$

For independent noise, $\varepsilon_{t,i}$, the bias of this estimator is $2\bar{n}\sigma^2_\varepsilon$, where $\bar{n} = n/L$, the average size of subsamples. The variance σ^2_ε can be consistently approximated using realized volatility computed with all the observations:

$$\hat{\sigma}^2_\varepsilon = \frac{1}{2n} RV^{(\text{all})}_t.$$

Then we obtain TSRV as

$$TSRV_t = RV^{(\text{avg})}_t - \frac{\bar{n}}{n} RV^{(\text{all})}_t, \tag{4}$$

which is an asymptotic unbiased estimator of integrated volatility. Zhang et al. (2005) and Aït-Sahalia and Mancini (2007) show the theoretical and empirical effectiveness of TSRV, respectively.

Furthermore, in the case of the dependent noise structure, Zhang (2006) and Aït-Sahalia, Mykland, and Zhang (2006) show that RV_t has a bias and a larger variance due to the noise. See, e.g., McAleer and Medeiros (2006) for a review of the effects of the microstructure noise.

Suppose that $r^*_{t,i}$ and $\nu_{t,i}$ in the equation (3) are uncorrelated. Then, taking the variance of the both sides of the equation (3), we have

$$\text{var}(r_{t,i}) = \text{var}(r^*_{t,i}) + \text{var}(\nu_{t,i}).$$

If the true price $p^*_{t,i}$ follows the equation (1), $\text{var}(r^*_{t,i})$ increases as the time interval increases. On the other hand, $\text{var}(\nu_{t,i})$ remains the same ($2\sigma^2_\varepsilon$ if $\varepsilon_{t,i}$ has a constant variance σ^2_ε independent of the time interval and no autocorrelation). This means that the effect of the microstructure noise decreases as the time interval increases. Hence, daily returns are less subject to the microstructure noise than intraday returns. But daily returns suffer from another source of noise due to the discretization while the realized volatility is less subject to the discretization noise, which shows that daily returns and realized volatility can complement each other. This motivates us to model daily returns and realized volatility simultaneously as in the next subsection, which allows us to avoid additional calculations for adjusting the realized volatility.

2.2. *Model*

2.2.1. *Stochastic Volatility*

In this subsection, we propose a new model which utilizes daily returns and the realized volatility simultaneously. The model is an extension of the well-known stochastic volatility (SV) model (see for example Taylor (1986), Shephard (1996), and Ghysels, Harvey, and Renault (1996)). A simple SV model is written as,

$$\begin{aligned} R_t &= \exp(h_t/2)\epsilon_t, \quad \epsilon_t \sim \mathrm{N}(0,1), \quad t = 1,\ldots,T, \\ h_{t+1} &= \mu + \phi(h_t - \mu) + \eta_t, \quad \eta_t \sim \mathrm{N}(0,\sigma_\eta^2), \quad t = 1,\ldots,T-1, \end{aligned} \tag{5}$$

and

$$h_1 = \mu + \eta_0, \quad \eta_0 \sim \mathrm{N}\left(0, \frac{\sigma_\eta^2}{1-\phi^2}\right),$$

where h_t is the latent log volatility (log integrated volatility) at time t. We denote the disturbance term in the equation of h_{t+1} in (5) as η_t following the literature on stochastic volatility models although it might be natural to denote it as η_{t+1} because it is the disturbance to h_{t+1}. Notice that even if we denote it as η_t, it is unobserved at time t. It is only R_t that is observed at time t.

For notational convenience, let $y_{1,t}$ and $y_{2,t}$ denote a daily return and a logarithm of realized volatility respectively. We extend the SV model as

$$\begin{aligned} y_{1,t} &= \exp(h_t/2)\epsilon_t, \quad \epsilon_t \sim \mathrm{N}(0,1), \\ y_{2,t} &= h_t + u_t, \quad u_t \sim \mathrm{N}(0,\sigma_u^2), \\ h_{t+1} &= \mu + \phi(h_t - \mu) + \eta_t, \quad \eta_t \sim \mathrm{N}(0,\sigma_\eta^2), \end{aligned} \tag{6}$$

and

$$h_1 = \mu + \eta_0, \quad \eta_0 \sim \mathrm{N}\left(0, \frac{\sigma_\eta^2}{1-\phi^2}\right),$$

which we call SV-RV model. Moreover, since the realized volatility can be biased due to the non-trading hours and microstructure noise, we modify the SV-RV model by adding the bias-correction term ξ in the second observation equation of (6), i.e.,

$$\begin{aligned} y_{1,t} &= \exp(h_t/2)\epsilon_t, \quad \epsilon_t \sim \mathrm{N}(0,1), \\ y_{2,t} &= \xi + h_t + u_t, \quad u_t \sim \mathrm{N}(0,\sigma_u^2), \\ h_{t+1} &= \mu + \phi(h_t - \mu) + \eta_t, \quad \eta_t \sim \mathrm{N}(0,\sigma_\eta^2), \end{aligned} \tag{7}$$

and

$$h_1 = \mu + \eta_0, \quad \eta_0 \sim \mathrm{N}\left(0, \frac{\sigma_\eta^2}{1-\phi^2}\right).$$

If ξ is positive, realized volatility has an upward bias that may be due to the market microstructure noise and if ξ is negative, it has a downward bias due to the non-trading hours. Therefore, we may observe the strength of effects of the microstructure noise and non-trading hours from the sign of ξ. We also call this model SV-RVC (SV-RV Corrected with respect to the bias due to the microstructure noise and non-trading hours) model.

The SV-RVC model can estimate the biases due to the both microstructure noise and non-trading hours simultaneously without the prior or two-step calculation for determining optimal time-interval of Bandi and Russell (2005), subsampling of Zhang et al. (2005), or scaling of Hansen and Lunde (2005). Further, SV-RV and SV-RVC models have a certain advantage in that they enable us to estimate the entire conditional predictive distribution of returns and hence common risk measures such as VaR and expected shortfall easily.

2.2.2. *Asymmetric Stochastic Volatility*

It is well known in stock markets that there is a negative correlation between today's return and tomorrow's volatility (see e.g. Black (1976) and Christie (1982)). To describe this asymmetry in volatility, we extend our model to the asymmetric stochastic volatility (ASV) model. The asymmetric SV-RVC (ASV-RVC) model is written as

$$\begin{aligned} y_{1,t} &= \exp(h_t/2)\epsilon_t, \\ y_{2,t} &= \xi + h_t + u_t, \\ h_{t+1} &= \mu + \phi(h_t - \mu) + \eta_t, \\ h_1 &= \mu + \eta_0, \quad \eta_0 \sim \mathrm{N}\left(0, \frac{\sigma_\eta^2}{1-\phi^2}\right), \end{aligned} \tag{8}$$

and

$$\begin{pmatrix} \epsilon_t \\ u_t \\ \eta_t \end{pmatrix} \sim \mathrm{N}\left(\begin{pmatrix} 0 \\ 0 \\ 0 \end{pmatrix}, \begin{pmatrix} 1 & 0 & \rho\sigma_\eta \\ 0 & \sigma_u^2 & 0 \\ \rho\sigma_\eta & 0 & \sigma_\eta^2 \end{pmatrix} \right). \tag{9}$$

The additional parameter ρ captures the correlation between $y_{1,t}$ and h_{t+1}. If $\rho < 0$, it is consistent with the above volatility asymmetry in stock markets.

2.3. *Markov Chain Monte Carlo Simulation*

We describe the estimation methods for the models without asymmetry in this subsection (see Appendix B for the models with asymmetry). Because of the nonlinear relation between the daily return and the log latent volatility in equations (5), (6), and (7), we cannot compute the likelihood of these models by Kalman filter. But given $h = (h_1, \ldots, h_T)$, we can compute the conditional likelihood of the SV-RVC model as

$$\begin{aligned} & f(y_{1,1}, y_{2,1}, \ldots, y_{1,T}, y_{2,T} | \theta, h) \\ &= \prod_{t=1}^{T} \frac{1}{\sqrt{2\pi}\exp(h_t/2)} \exp\left\{ -\frac{y_{1,t}^2}{2\exp(h_t)} \right\} \times \frac{1}{\sqrt{2\pi}\sigma_u} \exp\left\{ -\frac{(y_{2,t} - \xi - h_t)^2}{2\sigma_u^2} \right\}, \end{aligned}$$

where θ denotes the parameters. Hence, we take a Bayesian approach and estimate the posterior distribution of parameters in the SV, SV-RV, and SV-RVC models by considering h as additional latent variables. In this setup, the most important is how to sample h efficiently. Therefore, we first describe the sampling algorithm for h.

2.3.1. *Efficient Sampler for the Latent Volatilities*

There are various sampling methods for h such as the single-move sampler proposed by Jacquier, Polson, and Rossi (1994) or the mixture sampler by Kim, Shephard, and Chib (1998). But the single-move sampler is extremely inefficient and the mixture sampler requires us to approximate the distribution of $log(\epsilon_t^2)$ by a mixture of normal distributions. In this article, we use the block (multi-move) sampler proposed by Shephard and Pitt (1997) and Watanabe and Omori (2004).

To illustrate their block sampler, we consider the SV-RVC model. The observation equations of the model are

$$y_{1,t} = \exp(h_t/2)\epsilon_t, \quad \epsilon_t \sim \mathrm{N}(0,1),$$

and

$$y_{2,t} = \xi + h_t + u_t, \quad u_t \sim \mathrm{N}(0,\sigma_u^2), \tag{10}$$

while state equations are written as

$$h_{t+1} = (1-\phi)\mu + \phi h_t + \eta_t, \quad \eta_t \sim \mathrm{N}(0,\sigma_\eta^2), \tag{11}$$

and

$$h_1 = \mu + \eta_0, \quad \eta_0 \sim \mathrm{N}\left(0, \frac{\sigma_\eta^2}{1-\phi^2}\right).$$

To sample h from the posterior distribution, we divide $(h_1, \ldots, h_T)$ into $K+1$ blocks, $(h_{k_{j-1}+1}, \ldots, h_{k_j+1})'$, for $j = 0, \ldots, K+1$, with $k_0 = 0$ and $k_{K+1} = T$. The selection of K knots, $(k_1, \ldots, k_K)$, is implemented randomly and independently as

$$k_j = \mathrm{int}\{T \times (j + U_j)/(K+2)\}, \quad j = 1, \ldots, K,$$

where U_j's are independent uniforms in $[0,1]$ and "int" denotes integer part. Since we sample each block given parameters $\theta \equiv (\xi, \sigma_u^2, \mu, \phi, \sigma_\eta^2)$, other blocks, and observations $Y \equiv (y_1, \ldots, y_T)$ where $y_t \equiv (y_{1,t}, y_{2,t})$, this sampling method is called a block sampler or multi-move sampler (e.g. Shephard and Pitt (1997)).

Suppose that $k_{j-1} = t-1$ and $k_j = t+k$. Then we sample $h^{(j)} \equiv (h_t, h_{t+1}, \ldots, h_{t+k})$ given volatilities in other blocks, $(h_1, \ldots, h_{t-1}, h_{t+k+1}, \ldots, h_T)$, θ, and Y. Since $h^{(j)}$ only depends on h_{t-1}, h_{t+k+1}, $(y_t, \ldots, y_{t+k})$ and θ, it is enough to consider sampling from the posterior distribution,

$$f(h^{(j)}|h_{t-1}, h_{t+k+1}, y_t, \ldots, y_{t+k}, \theta).$$

Given h_{t-1}, h_{t+k+1}, $(y_t, \ldots, y_{t+k})$ and θ, we can compute $h^{(j)}$ from $\eta^{(j)} \equiv (\eta_{t-1}, \ldots, \eta_{t+k-1})$ using equation (11). Thus, we consider sampling $\eta^{(j)}$ from the posterior distribution,

$$f(\eta^{(j)}|h_{t-1}, h_{t+k+1}, y_t, \ldots, y_{t+k}, \theta). \tag{12}$$

To construct a proposal distribution for the Metropolis-Hastings (MH) algorithm, we approximate this posterior density by the corresponding density of the linear Gaussian state space model (see Appendix A for details) given by

$$\begin{aligned} \hat{y}_{1,s} &= h_s + \hat{\epsilon}_{1,s}, \quad \hat{\epsilon}_{1,s} \sim \mathrm{N}(0, v_s), \\ y_{2,s} &= \xi + h_s + u_s, \quad u_s \sim \mathrm{N}(0, \sigma_u^2), \end{aligned} \tag{13}$$

and

$$h_{s+1} = \mu + \phi(h_s - \mu) + \eta_s, \quad \eta_s \sim \mathrm{N}(0, \sigma_\eta^2),$$

where $\hat{y}_{1,s}$ and v_s are defined as,

(i) if $s = t, t+1, \ldots, t+k-1$ or $s = t+k = T$,

$$\hat{y}_{1,s} = \hat{h}_s + v_s l'(\hat{h}_s), \quad v_s = -\frac{1}{l''(\hat{h}_s)},$$

(ii) if $s = t+k < T$,

$$\hat{y}_s = \hat{h}_s + v_s\left[l'(\hat{h}_s) + \frac{\phi}{\sigma_\eta^2}\left\{h_{t+k+1} - \mu - \phi(\hat{h}_s - \mu)\right\}\right], \quad v_s = \frac{\sigma_\eta^2}{\phi^2 - \sigma_\eta^2 l''(\hat{h}_s)},$$

for some $\hat{h}_s$. We denote the posterior density of the $\eta^{(j)}$ from this linear Gaussian state space model by $g(\eta^{(j)})$.

We sample $\eta^{(j)}$ from the posterior density g using the simulation smoother of de Jong and Shephard (1995) and Durbin and Koopman (2002). But since g is the approximate density for the posterior density f, we use the acceptance-rejection Metropolis-Hasting (ARMH) algorithm proposed by Tierney (1994) (see also Chib and Greenberg (1995)) for sampling from f. We choose $\hat{h}_s$ as the posterior mode, which is calculated from the mode of $\eta^{(j)}$. In order to calculate the mode, $\hat{\eta}^{(j)}$, we first apply the disturbance smoother of Koopman (1993) with a starting value of $\hat{\eta}^{(j)}$. Using the obtained $\hat{\eta}^{(j)}$, we apply the disturbance smoother again. After some iterations, we can obtain the approximate mode of $\eta^{(j)}$ (see e.g. Shephard and Pitt (1997)).

2.3.2. *Sampling Parameters*

For the SV-RVC model in (7), we set priors as

$$\xi \sim \mathrm{N}(m_\xi, s_\xi^2), \quad \sigma_u^2 \sim \mathrm{IG}\left(\frac{n_u}{2}, \frac{d_u}{2}\right), \quad \mu \sim \mathrm{N}(m_\mu, s_\mu^2), \quad \frac{1+\phi}{2} \sim \mathrm{Beta}(a,b), \quad \sigma_\eta^2 \sim \mathrm{IG}\left(\frac{n_\eta}{2}, \frac{d_\eta}{2}\right).$$

Then, denoting $Y_1 = (y_{1,1}, \ldots, y_{1,T})$ and $Y_2 \equiv (y_{2,1}, \ldots, y_{2,T})$, the posterior density for $\theta \equiv (\xi, \sigma_u^2, \mu, \phi, \sigma_\eta^2)$ and h becomes

$$\begin{aligned} f(\theta, h|Y_1, Y_2) \propto & \exp\left[-\frac{1}{2}\sum_{t=1}^T \left\{h_t - y_{1,t}^2 \exp(-h_t)\right\}\right] (\sigma_u^2)^{-T/2} \exp\left\{-\frac{1}{2\sigma_u^2}\sum_{t=1}^T (y_{2,t} - \xi - h_t)^2\right\} \\ & \times \sqrt{1-\phi^2}(\sigma_\eta^2)^{-T/2} \exp\left\{-\frac{1}{2\sigma_\eta^2}(1-\phi^2)(h_1-\mu)^2 - \sum_{t=1}^{T-1}(h_{t+1} - (1-\phi)\mu - \phi h_t)^2\right\} \\ & \times \exp\left\{-\frac{(\xi - m_\xi)^2}{2s_\xi^2}\right\} (\sigma_u^2)^{-(n_u/2+1)} \exp\left(-\frac{d_u}{2\sigma_u^2}\right) \exp\left\{-\frac{(\mu - m_\mu)^2}{2s_\mu^2}\right\} \\ & \times \left(\frac{1+\phi}{2}\right)^{a-1} \left(\frac{1-\phi}{2}\right)^{b-1} (\sigma_\eta^2)^{-(n_\eta/2+1)} \exp\left(-\frac{d_\eta}{2\sigma_\eta^2}\right). \end{aligned}$$

To implement the Markov chain Monte Carlo simulation, we sample from the posterior distribution as follows:

1. Simulate h from $f(h|\mu, \phi, \sigma_\eta^2, Y_1, Y_2)$.
2. Simulate ξ from $f(\xi|\sigma_u^2, h, Y_2)$.
3. Simulate σ_u^2 from $f(\sigma_u^2|\xi, h, Y_2)$.
4. Simulate μ from $f(\mu|\phi, \sigma_\eta^2, h)$.
5. Simulate σ_η^2 from $f(\sigma_\eta^2|\mu, \phi, h)$.
6. Simulate ϕ from $f(\phi|\mu, \sigma_\eta^2, h)$.

We note that ξ and σ_u^2 only depend on the observation equation (10) given h while μ, ϕ, and σ_η^2 only depend on the volatility equation (11) given h.

In the first step, we conduct the multi-move sampler described in the previous subsection. In the second and third steps, we sample from the conditional posterior distributions of ξ and σ_η^2,

$$\xi|\sigma_u^2, Y_2, h \sim \mathrm{N}(\tilde{m}_\xi, \tilde{s}_\xi^2), \quad \sigma_u^2|\xi, Y_2, h \sim \mathrm{IG}\left(\frac{\tilde{n}_u}{2}, \frac{\tilde{d}_u}{2}\right),$$

where

$$\tilde{m}_\xi = \frac{s_\xi^2(y_{2,t} - h_t) + \sigma_u^2 m_\xi}{T s_\xi^2 + \sigma_u^2}, \quad \tilde{s}_\xi^2 = \frac{s_\xi^2 \sigma_u^2}{T s_\xi^2 + \sigma_u^2}, \quad \tilde{n}_u = T + n_u, \quad \tilde{d}_u = d_u + \sum_{t=1}^T (y_{2,t} - \xi - h_t)^2.$$

In the fourth and fifth steps, we generate samples from the conditional posterior distributions of μ and σ_η^2,

$$\mu|\phi, \sigma_\eta^2, h \sim \mathrm{N}(\tilde{m}_\mu, \tilde{s}_\mu^2), \quad \sigma_\eta^2|\mu, \phi, h \sim \mathrm{IG}\left(\frac{\tilde{n}_\eta}{2}, \frac{\tilde{d}_\eta}{2}\right),$$

where

$$\tilde{m}_\mu = \tilde{s}_\mu^2 \left\{ \frac{(1-\phi^2)}{\sigma_\eta^2} h_1 + \frac{(1-\phi)}{\sigma_\eta^2} \sum_{t=1}^{T-1} (h_{t+1} - \phi h_t) + \frac{m_\mu}{s_\mu^2} \right\},$$

$$\tilde{s}_\mu^2 = \frac{s_\mu^2 \sigma_\eta^2}{s_\mu^2 \{(T-1)(1-\phi)^2 + 1 - \phi^2\} + \sigma_\eta^2},$$

$$\tilde{n}_\eta = T + n_\eta,$$

and

$$\tilde{d}_\eta = d_\eta + (h_1 - \mu)^2 (1 - \phi^2) + \sum_{t=1}^{T-1} \{h_{t+1} - \mu - \phi(h_t - \mu)\}^2.$$

In the final step, the logarithm of the posterior density is

$$\log f(\phi|\mu, \sigma_\eta^2, h_1, \ldots, h_T) = \text{const.} + \log\{\varphi(\phi)\} - \frac{1}{2\sigma_\eta^2} \sum_{t=1}^{T-1} \{h_{t+1} - \mu - \phi(h_t - \mu)\}^2,$$

where $|\phi| < 1$ and

$$\log \varphi(\phi) = (a-1)\log(1+\phi) + (b-1)\log(1-\phi) - \frac{(h_1 - \mu)^2(1-\phi^2)}{2\sigma_\eta^2} + \frac{1}{2}\log(1-\phi^2).$$

In order to sample from this density, we employ MH algorithm (Chib and Greenberg (1995)). We construct the proposal density $h(\phi)$ as an approximation to the conditional posterior density by omitting the term $\log \varphi(\phi)$, i.e.,

$$\begin{aligned} \log f(\phi|\mu, \sigma_\eta^2, h_1, \ldots, h_T) &\approx \text{const.} - \frac{1}{2\sigma_\eta^2} \sum_{t=1}^{T-1} \{h_{t+1} - \mu - \phi(h_t - \mu)\}^2 \\ &= \text{const.} - \frac{(\phi - m_\phi)^2}{2 s_\phi^2} \\ &= \text{const.} + \log h(\phi), \end{aligned}$$

where

$$m_\phi = \frac{\sum_{t=1}^{T-1} (h_{t+1} - \mu)(h_t - \mu)}{\sum_{t=1}^{T-1} (h_t - \mu)^2}, \quad s_\phi^2 = \frac{\sigma_\eta^2}{\sum_{t=1}^{T-1} (h_t - \mu)^2}.$$

If ϕ_{j-1} is a current sample of ϕ, we propose a candidate ϕ^p for ϕ_j by sampling from $\mathrm{N}(m_\phi, s_\phi^2)$ truncated on $(-1, 1)$ and accepting it with probability

$$q = \min\left\{ \frac{f(\phi^p) h(\phi_{j-1})}{f(\phi_{j-1}) h(\phi^p)}, 1 \right\} = \min\left\{ \frac{\varphi(\phi^p)}{\varphi(\phi_{j-1})}, 1 \right\}.$$

3. Application to Stock Return Data

3.1. *Data and Realized Volatility*

We use the high frequency data of Tokyo stock price index (TOPIX) obtained from the Nikkei NEEDS MT tick data during the period from April 1, 1996 to March 31, 2005 (2216 trading days). For this period, the highest frequency at which the price is preserved is one minute. TSE is open for 9:00-11:00 (morning session) and 12:30-15:00 (afternoon session) in usual trading days and only for 9:00-11:00 in the first and

Fig. 1. Realized volatilities calculated from 1-minute intraday returns (RV^1, top left), 5-minute (RV^5, top right), and 10-minute (RV^{10}, and two-scale realized volatility ($TSRV$, bottom right) during the period from April 1, 1996 to March 31, 2005 (2216 trading days).

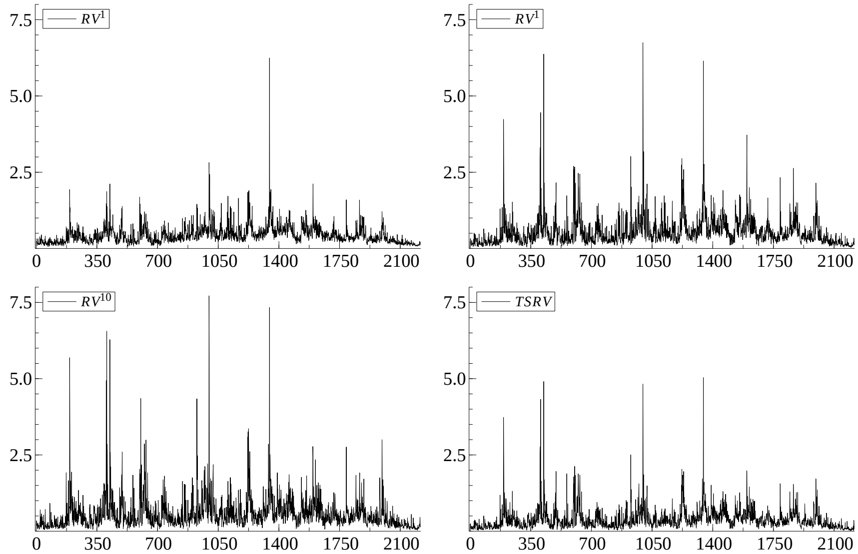

last trading days in every year. Excluding the overnight and lunch time intervals, we obtain 119 intraday returns in the morning session and 149 returns in the afternoon session.

To confirm that SV-RVC model can correct the bias due to market microstructure noise and non-trading hours, we use the realized volatilities calculated from 1-, 5-, and 10-minute intraday returns when the market is open. We compute RV_t^m by omitting the overnight and lunch time interval return (we also compute RV_t^m in the first and last trading days in every year using only morning session returns), where $m = 1, 5, 10$ denote the time interval used for calculating realized volatilities. Additionally, we compute TSRV in (4) using RV_t^1 as $RV_t^{(\mathrm{all})}$ and $RV_t^{5(j)}$ $(j = 1, \ldots, 5)$ as subsample realized volatilities. Following Hansen and Lunde (2005), we calculate scaled realized volatilities as,

$$SRV_t = cRV_t, \quad c = \frac{\sum_{t=1}^{T}(R_t - \bar{R})^2}{\sum_{t=1}^{T} RV_t}.$$

Values of c are 3.6711, 2.9645, 2.7881, and 4.0720 for RV_t^1, RV_t^5, RV_t^{10}, and $TSRV_t$, respectively. Since all these values are smaller than $24/4.5 = 5.3333$, we confirm that non-trading hours contribute to the increase in volatility less than trading hours, which is consistent with previous findings (Fama (1965), French and Roll (1986), and Nelson (1991)).

Figures 1 - 4 are the realized volatilities at the time interval $m = 1, 5, 10$ (minute) and TSRV using intraday returns only when the market is open (RV), scaled ones (SRV), and their logarithms ($\log(RV)$, $\log(SRV)$). Figure 5 plots daily return (R), its absolute value ($|R|$), squared return (R^2), and its logarithm ($\log R^2$). They show that the variation of realized volatilities is smaller than that of squared daily return, which is due to the discretization noise in daily returns.

Tables 1 - 3 show descriptive statistics. We observe four interesting results from this table. First, the mean of RV^m $(m = 1, 5, 10)$ and $TSRV$ is smaller than that of the squared daily return, which implies there is a negative bias in the realized volatility due to non-trading hours. We also observe that the mean of RV^m $(m = 1, 5, 10)$ decreases as the sampling frequency increases from 10- to 1-minute, which is opposite to our expectation that RV^m increases as the sampling frequency increases due to microstructure noise. But this results may happen as in the volatility signature plots in Hansen and Lunde (2006). For example, in the upper right of Figure 1 of Hansen and Lunde (2006), average realized volatility decreases as the sampling

Fig. 2. Scaled realized volatilities calculated from 1-minute intraday returns (SRV^1, top left), 5-minute (SRV^5, top right), and 10-minute (SRV^{10}, and scaled two-scale realized volatility ($STSRV$, bottom right) during the period from April 1, 1996 to March 31, 2005 (2216 trading days).

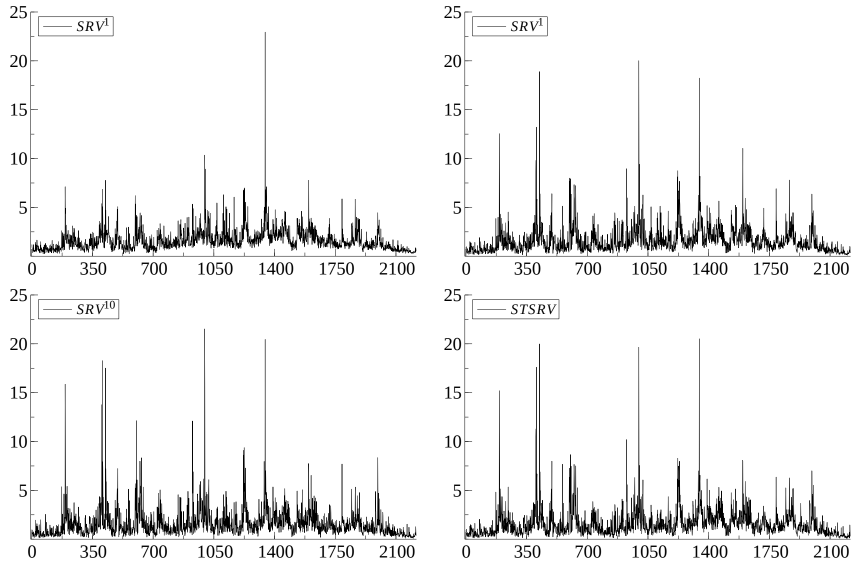

Fig. 3. Logarithm of realized volatilities calculated from 1-minute intraday returns ($\log(RV^1)$, top left), 5-minute ($\log(RV^5)$, top right), and 10-minute ($\log(RV^{10})$, and that of two-scale realized volatility ($\log(TSRV)$, bottom right) during the period from April 1, 1996 to March 31, 2005 (2216 trading days).

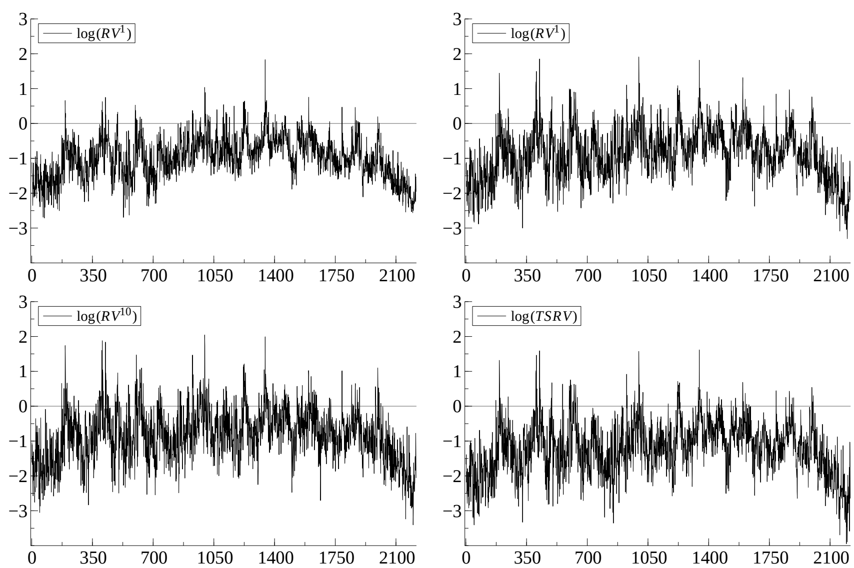

frequency increases from 10- to 1-minute and turns to increase from 30- to 1-second. Therefore, we consider that this phenomenon is due to the limited frequency of our data. The standard deviation of the realized volatilities is much smaller than the squared return as we expected from Figures 1 and 5.

Second, the standard deviation of RV^m becomes larger as the time interval m increases, which confirms the intraday return becomes noisy due to the discretization effect as the interval increases. These results suggest that the more precise estimate of the true volatility may be obtained by correcting the bias due to

Table 1
Descriptive statistics for realized volatilities for the market open period (RV^m, $TSRV$) and scaled realized volatilities (SRV^m, $STSRV$), at frequency $m = 1, 5, 10$ (minute) during the period from 1 April 1996 to 31 March 2005 (2216 trading days). LB(10) is the heteroskedasticity-corrected Ljung-Box statistics of Diebold (1988) with 10 lags. The critical values for LB_{10} are: 15.99 (10%), 18.31 (5%), and 23.21 (1%).

	RV^1	RV^5	RV^{10}	$TSRV$
Mean	0.4424	0.5478	0.5825	0.3988
Stdev	0.3089	0.4923	0.5722	0.3756
Skewness	4.6566	4.3165	4.7976	4.6667
Kurtosis	64.2218	38.3029	42.8742	43.1197
Max	6.2472	6.7510	7.7187	5.0358
Min	0.0665	0.0367	0.0332	0.0194
LB(10)	1294.09	1095.32	751.79	1000.46
	SRV^1	SRV^5	SRV^{10}	$STSRV$
Mean	1.6240	1.6240	1.6240	1.6240
Stdev	1.1340	1.4595	1.5955	1.5295
Skewness	4.6566	4.3165	4.7976	4.6667
Kurtosis	64.2218	38.3029	42.8742	43.1197
Max	22.9340	20.0133	21.5208	20.5057
Min	0.2440	0.1087	0.0927	0.0788
LB(10)	1294.09	1095.32	751.79	1000.46

Table 2
Descriptive statistics for logarithm of realized volatilities for the market open period ($\log(RV^m)$, $\log(TSRV)$) and scaled realized volatilities ($\log(SRV^m)$, $\log(STSRV)$), at frequency $m = 1, 5, 10$ (minute) during the period from 1 April 1996 to 31 March 2005 (2216 trading days). LB(10) is the heteroskedasticity-corrected Ljung-Box statistics of Diebold (1988) with 10 lags. The critical values for LB_{10} are: 15.99 (10%), 18.31 (5%), and 23.21 (1%).

	$\log(RV^1)$	$\log(RV^5)$	$\log(RV^{10})$	$\log(TSRV)$
Mean	−0.9940	−0.8739	−0.8395	−1.2087
Stdev	0.5937	0.7350	0.7643	0.7606
Skewness	0.0157	−0.0256	0.0250	−0.0756
Kurtosis	3.1601	3.2047	3.2493	3.3252
Max	1.8321	1.9097	2.0436	1.6166
Min	−2.7111	−3.3061	−3.4043	−3.9448
LB(10)	4875.28	4044.76	3359.10	3730.37
	$\log(SRV^1)$	$\log(SRV^5)$	$\log(SRV^{10})$	$\log(STSRV)$
Mean	0.3065	0.2128	0.1859	0.1954
Stdev	0.5937	0.7350	0.7643	0.7606
Skewness	0.0157	−0.0256	0.0250	−0.0756
Kurtosis	3.1601	3.2047	3.2493	3.3252
Max	3.1326	2.9964	3.0690	3.0207
Min	−1.4106	−2.2194	−2.3789	−2.5407
LB(10)	4875.28	4044.76	3359.10	3730.37

Fig. 4. Logarithm of scaled realized volatilities calculated from 1-minute intraday returns ($\log(SRV^1)$, top left), 5-minute ($\log(SRV^5)$, top right), and 10-minute ($\log(SRV^{10})$, and that of scaled two-scale realized volatility ($\log(STSRV)$, bottom right) during the period from April 1, 1996 to March 31, 2005 (2216 trading days).

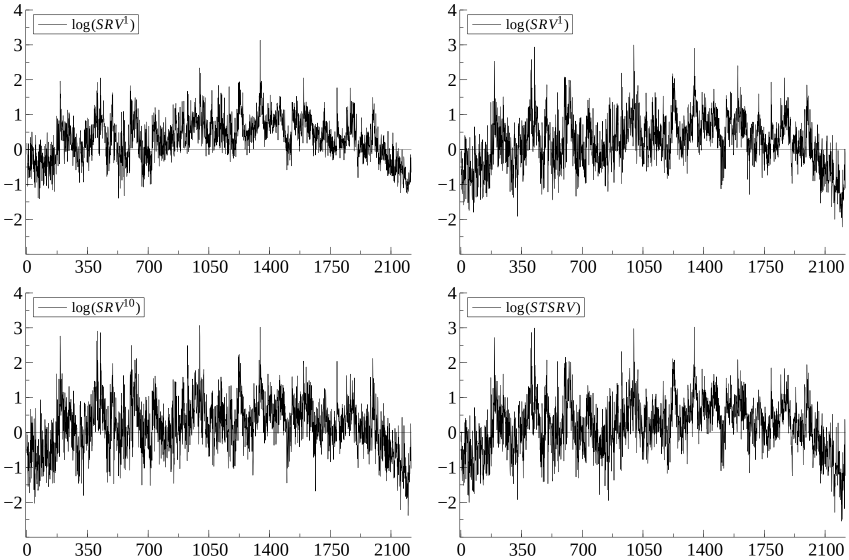

Fig. 5. daily return (R, top left), its absolute value ($|R|$, top right), squared return (R^2, bottom left), and its logarithm ($\log R^2$, bottom right) during the period from April 1, 1996 to March 31, 2005 (2216 trading days).

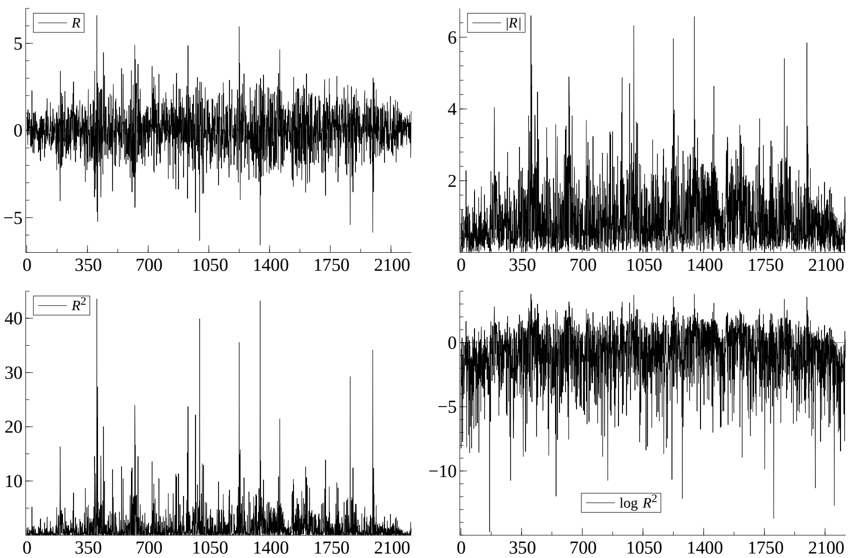

non-trading hours and microstructure noise in RV^1.

Third, the skewness and kurtosis indicate that the realized volatilities are not Gaussian but their logarithms are nearly Gaussian, which motivates us to model the logarithm of realized volatilities instead of the realized volatilities. Finally, LB(10), the heteroskedasticity-corrected Ljung-Box statistic including 10 lags calculated following Diebold (1988), shows that daily return is not autocorrelated while volatilities, especially the log realized volatilities, are autocorrelated significantly at the one percent level. This result is consistent with the well-known phenomenon of volatility clustering.

Table 3
Descriptive statistics daily return (R), its absolute value ($|R|$), squared return (R^2), and log of them ($\log|R|$, $\log R^2$) during the period from 1 April 1996 to 31 March 2005 (2216 trading days). LB(10) is the heteroskedasticity-corrected Ljung-Box statistics of Diebold (1988) with 10 lags. The critical values for LB_{10} are: 15.99 (10%), 18.31 (5%), and 23.21 (1%).

	R	$\|R\|$	R^2	$\log\|R\|$	$\log R^2$
Mean	−0.0147	0.9573	1.6242	−0.5046	−1.0091
Stdev	1.2744	0.8413	3.2096	1.1353	2.2707
Skewness	−0.1084	1.7813	6.0007	−1.2009	−1.2009
Kurtosis	4.9005	8.2747	57.9221	5.6049	5.6049
Max	6.5993	6.5993	43.5513	1.8870	3.7739
Min	−6.5736	0.0006	0.0000	−7.3682	−14.7364
LB(10)	20.42	189.96	100.81	73.45	73.45

These findings are in accordance with previous studies: Andersen, Bollerslev, Diebold, and Labys (2001b) for exchange rates; Andersen, Bollerslev, Diebold, and Ebens (2001a) for stocks; Martens (2002) for stock index futures; and Watanabe (2007) for Japanese stock index (Nikkei 225).

3.2. *Estimation Results*

Tables 4 - 7 summarize MCMC estimation results of SV, SV-RV, and SV-RVC models obtained by 5000 samples recorded after discarding 1000 samples from MCMC iterations (all calculations in this paper are done by using Ox (Doornik (2002))). We apply the latter two models to both realized volatilities for the market open period (RV^m, $TSRV$) and scaled one (SRV^m, $STSRV$) at each time interval ($m = 1, 5, 10$) and denote models using scaled realized volatilities as SV-SRV and SV-SRVC models. CD is the p-value of the convergence diagnostic (CD) test by Geweke (1992). The inefficiency factor is defined as $1 + 2\sum_{s=1}^{\infty}\rho_s$, where ρ_s is the sample autocorrelation at lag s, and is computed to measure how well the MCMC chain mixes (see e.g. Chib (2001)). It is the ratio of the numerical variance of the posterior sample mean to the variance of the posterior sample mean from uncorrelated draws. The inverse of inefficiency factor is also known as relative numerical efficiency (Geweke (1992)). When the inefficiency factor is equal to x, we need to draw MCMC samples x times as many as uncorrelated samples to obtain the same accuracy.

Table 4 shows that ϕ is estimated relatively lower in the SV-RV models using RV^m and $TSRV$ although ϕ is expected to be close to one as a result of the strong autocorrelations of log realized volatilities. Since ϕ is close to one in the SV-RVC, SV-SRV, and SV-SRVC models in Tables 5, 6, and 7, this is probably because the bias is not corrected appropriately for the non-trading hours.

In Table 5, the posterior means of ξ in the SV-RVC models are all negative. This implies that the effect of non-trading hours is stronger than that of microstructure noise. We note that the posterior mean of $\xi = -1.2334$ in the SV-RVC model using RV^1 is larger than the scaling factor, $-\log(c) = -1.3005$, and, further, the posterior probability that ξ is positive is greater than 0.95 in the SV-SRVC model using SRV^1 in Table 7. From these results, we observe that the bias due to the microstructure noise still exists even after scaling, which means that correcting the bias due to non-trading hours is not sufficient for adjusting the total bias in the realized volatility. We also note that the difference between -1.2334 and -1.3005 is 0.0671 which is almost equal to the posterior mean of $\xi = 0.0670$ in SV-SRVC model in Table 7.

Table 7 shows that 95% credible intervals of ξ contain zeros for the SV-SRVC models using SRV^5 and SRV^{10}. This result shows that the bias due to the microstructure noise disappears as the time interval m increases. On the contrary, the variances of realized volatility (σ_u^2) increases as m increases. This bias-variance trade-off is consistent with previous studies such as Bandi and Russell (2005) and Hansen and Lunde (2006). While these studies suggest taking the optimal time interval for dealing with this trade-off, our SV-RVC model can correct the bias without considering a selection of such a time interval. Additionally, we observe from Table 7 that $TSRV$ can adjust the bias due to the microstructure noise but the variances, σ_u^2, is larger than that of RV^1. Therefore, the model provides volatility estimator with the least variation

Table 4
Estimation results of SV-RV model using realized volatilities. The last two columns are p-value of Geweke's convergence diagnostic (CD) test and inefficiency factor, respectively. Priors are set as $\sigma_u^2 \sim \mathrm{IG}(5/2, 0.05/2)$, $\mu \sim \mathrm{N}(0,1)$, $(1+\phi)/2 \sim$ Beta(20, 1.5), and $\sigma_\eta^2 \sim \mathrm{IG}(5/2, 0.05/2)$.

		Mean	Stdev	95% interval	CD	Inef.
SV-RV	σ_u^2	0.0769	0.0056	[0.0661, 0.0876]	0.91	14.4
(RV^1)	μ	−0.9206	0.0478	[−1.0129, −0.8260]	0.47	0.9
	ϕ	0.8799	0.0151	[0.8490, 0.9079]	0.82	12.9
	σ_η^2	0.0722	0.0071	[0.0591, 0.0869]	0.49	23.2
SV-RV	σ_u^2	0.1344	0.0085	[0.1181, 0.1512]	0.38	7.6
(RV^5)	μ	−0.7763	0.0566	[−0.8865, −0.6642]	0.80	0.8
	ϕ	0.8735	0.0148	[0.8442, 0.9022]	0.83	7.1
	σ_η^2	0.1086	0.0101	[0.0894, 0.1290]	0.76	13.8
SV-RV	σ_u^2	0.1939	0.0108	[0.1724, 0.2150]	0.95	12.4
(RV^{10})	μ	−0.7097	0.0579	[−0.8237, −0.5948]	0.32	1.7
	ϕ	0.8809	0.0151	[0.8509, 0.9090]	0.81	13.0
	σ_η^2	0.1022	0.0108	[0.0829, 0.1255]	0.73	21.7
SV-RV	σ_u^2	0.2499	0.0145	[0.2227, 0.2789]	0.13	10.1
($TSRV$)	μ	−0.9652	0.0628	[−1.0886, −0.8395]	0.81	1.0
	ϕ	0.8868	0.0152	[0.8559, 0.9147]	0.77	15.4
	σ_η^2	0.1019	0.0115	[0.0813, 0.1266]	0.66	27.4

by using the realized volatility calculated from intraday returns of the shortest interval (one minute).

Figure 6 is the plots of posterior means with 95% credible intervals of the estimated h_t's under SV-RV and SV-SRVC models using RV^1. From the figure, we confirm that the bias due to non-trading hours largely affects the estimate of h_t. The results using the other realized volatilities are omitted because they are similar to the result using RV^1. Table 8 is the summary statistics of the estimated h_t's for $t = 0.2T$ (January 20, 1998) under SV-RV, SV-RVC, SV-SRV, and SV-SRVC models. We confirm from this table that SV-RV models underestimate h_t due to non-trading hours and that correcting the bias due to microstructure noise slightly affects the estimates. We obtain the same results for other several dates and thus omit the results.

We also compute the simultaneous model with asymmetry. Since we have already observed that the bias correction term is essential for our simultaneous model, we only estimate ASV-RVC models. Tables 9 and 10 show summary statistics of MCMC samples. Since 95% credible interval for ρ is below 0 for all models, the posterior probability that ρ is negative is greater than 0.95. It shows the importance of asymmetry in the stochastic volatility model, which is consistent with many previous studies.

To investigate the effect of lunch time non-trading hours, we also estimate the models using realized volatilities and scaled ones calculated from intraday returns including the lunch time interval. The results are the same as those when we used realized volatilities calculated without the lunch time interval and hence are omitted.

Table 5
Estimation results of SV-RVC model using realized volatilities. The last two columns are p-value of Geweke's convergence diagnostic (CD) test and inefficiency factor, respectively. Priors are set as $\xi \sim \mathrm{N}(0, 10)$, $\sigma_u^2 \sim \mathrm{IG}(5/2, 0.05/2)$, $\mu \sim \mathrm{N}(0, 1)$, $(1+\phi)/2 \sim \mathrm{Beta}(20, 1.5)$, and $\sigma_\eta^2 \sim \mathrm{IG}(5/2, 0.05/2)$.

		Mean	Stdev	95% interval	CD	Inef.
SV-RVC	ξ	−1.2334	0.0307	[−1.2908, −1.1725]	0.59	35.6
(RV^1)	σ_u^2	0.0931	0.0047	[0.0841, 0.1026]	0.06	39.8
	μ	0.2285	0.0795	[0.0703, 0.3840]	0.86	5.5
	ϕ	0.9517	0.0097	[0.9307, 0.9701]	0.11	39.7
	σ_η^2	0.0259	0.0040	[0.0187, 0.0347]	0.11	76.1
SV-RVC	ξ	−1.0707	0.0324	[−1.1341, −1.0057]	0.25	33.4
(RV^5)	σ_u^2	0.1467	0.0080	[0.1317, 0.1627]	0.27	20.5
	μ	0.1899	0.0785	[0.0375, 0.3478]	0.11	6.7
	ϕ	0.9294	0.0118	[0.9053, 0.9509]	0.22	20.7
	σ_η^2	0.0560	0.0078	[0.0418, 0.0717]	0.17	33.6
SV-RVC	ξ	−1.0425	0.0342	[−1.1102, −0.9761]	0.84	22.7
(RV^{10})	σ_u^2	0.1864	0.0099	[0.1675, 0.2064]	0.40	15.5
	μ	0.1954	0.0752	[0.0459, 0.3441]	0.58	4.8
	ϕ	0.9193	0.0129	[0.8931, 0.9440]	0.60	20.2
	σ_η^2	0.0641	0.0088	[0.0472, 0.0816]	0.61	32.2
SV-RVC	ξ	−1.4178	0.0309	[−1.4809, −1.3610]	0.46	21.0
($TSRV$)	σ_u^2	0.1709	0.0093	[0.1526, 0.1891]	0.28	40.9
	μ	0.1996	0.0798	[0.0418, 0.3552]	0.65	3.1
	ϕ	0.9308	0.0122	[0.9053, 0.9533]	0.38	34.4
	σ_η^2	0.0563	0.0084	[0.0408, 0.0739]	0.31	61.0

Fig. 6. Plots of posterior means with 95% credible intervals of the estimated h_t's under SV-RV (left) and SV-SRVC (right) models using RV^1 during the period from April 1, 1996 to March 31, 2005 (2216 trading days).

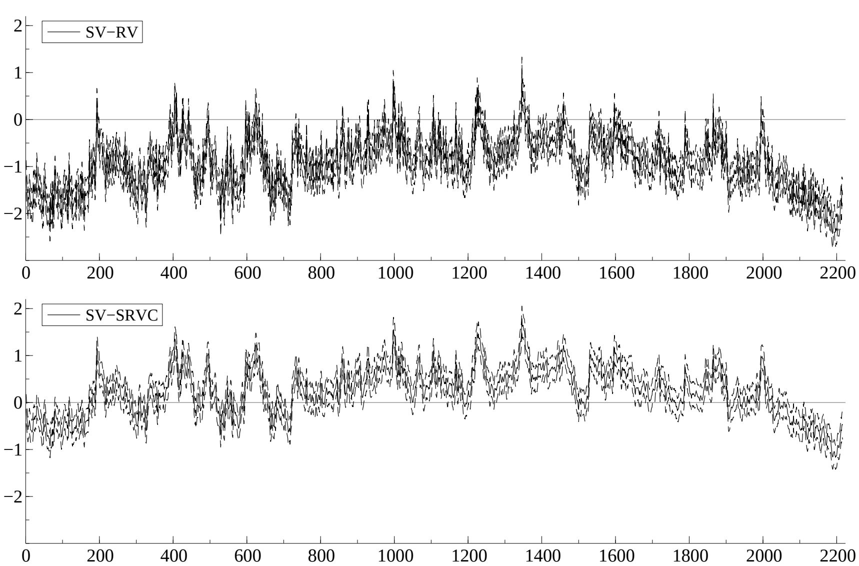

Table 6
Estimation results of SV-SRV model using scaled realized volatilities. The last two columns are p-value of Geweke's convergence diagnostic (CD) test and inefficiency factor, respectively. Priors are set as $\sigma_u^2 \sim \mathrm{IG}(5/2, 0.05/2)$, $\mu \sim \mathrm{N}(0,1)$, $(1+\phi)/2 \sim \mathrm{Beta}(20, 1.5)$, and $\sigma_\eta^2 \sim \mathrm{IG}(5/2, 0.05/2)$.

		Mean	Stdev	95% interval	CD	Inef.
SV-SRV	σ_u^2	0.0949	0.0046	[0.0858, 0.1041]	0.59	14.7
(SRV^1)	μ	0.2915	0.0760	[0.1414, 0.4418]	0.95	0.8
	ϕ	0.9549	0.0090	[0.9370, 0.9715]	0.52	14.8
	σ_η^2	0.0241	0.0037	[0.0169, 0.0318]	0.53	33.9
SV-SRV	σ_u^2	0.1464	0.0082	[0.1309, 0.1630]	0.89	30.8
(SRV^5)	μ	0.2043	0.0728	[0.0616, 0.3467]	0.97	0.5
	ϕ	0.9292	0.0122	[0.9042, 0.9510]	0.75	27.8
	σ_η^2	0.0561	0.0083	[0.0419, 0.0739]	0.75	48.6
SV-SRV	σ_u^2	0.1871	0.0106	[0.1661, 0.2081]	0.54	40.3
(SRV^{10})	μ	0.1803	0.0694	[0.0440, 0.3160]	0.31	0.6
	ϕ	0.9205	0.0146	[0.8892, 0.9471]	0.75	45.2
	σ_η^2	0.0632	0.0104	[0.0450, 0.0865]	0.74	65.7
SV-SRV	σ_u^2	0.1686	0.0089	[0.1509, 0.1861]	0.60	38.5
($STSRV$)	μ	0.1897	0.0737	[0.0445, 0.3349]	0.06	1.1
	ϕ	0.9282	0.0120	[0.9039, 0.9504]	0.25	37.9
	σ_η^2	0.0589	0.0081	[0.0446, 0.0768]	0.29	70.0

Table 7
Estimation results of SV-SRVC model using scaled realized volatilities. The last two columns are p-value of Geweke's convergence diagnostic (CD) test and inefficiency factor, respectively. Priors are set as $\xi \sim \mathrm{N}(0,10)$, $\sigma_u^2 \sim \mathrm{IG}(5/2, 0.05/2)$, $\mu \sim \mathrm{N}(0,1)$, $(1+\phi)/2 \sim \mathrm{Beta}(20, 1.5)$, and $\sigma_\eta^2 \sim \mathrm{IG}(5/2, 0.05/2)$.

		Mean	Stdev	95% interval	CD	Inef.
SV-SRVC	ξ	0.0670	0.0307	[0.0097, 0.1279]	0.59	35.5
(SRV^1)	σ_u^2	0.0931	0.0047	[0.0841, 0.1026]	0.06	39.8
	μ	0.2286	0.0795	[0.0703, 0.3842]	0.86	5.5
	ϕ	0.9517	0.0097	[0.9307, 0.9701]	0.11	39.7
	σ_η^2	0.0259	0.0040	[0.0187, 0.0347]	0.11	76.1
SV-SRVC	ξ	0.0132	0.0350	[−0.0513, 0.0808]	0.55	61.6
(SRV^5)	σ_u^2	0.1483	0.0083	[0.1316, 0.1642]	0.75	42.5
	μ	0.1908	0.0811	[0.0323, 0.3521]	0.59	12.4
	ϕ	0.9314	0.0122	[0.9056, 0.9531]	0.66	49.1
	σ_η^2	0.0540	0.0084	[0.0397, 0.0731]	0.99	77.0
SV-SRVC	ξ	−0.0215	0.0339	[−0.0883, 0.0435]	0.44	20.6
(SRV^{10})	σ_u^2	0.1889	0.0101	[0.1696, 0.2092]	0.81	28.1
	μ	0.1987	0.0767	[0.0451, 0.3527]	0.96	3.9
	ϕ	0.9231	0.0129	[0.8968, 0.9474]	0.94	29.9
	σ_η^2	0.0609	0.0089	[0.0445, 0.0788]	0.97	49.2
SV-SRVC	ξ	−0.0127	0.0333	[−0.0792, 0.0509]	0.20	21.5
($STSRV$)	σ_u^2	0.1696	0.0094	[0.1510, 0.1880]	0.99	24.8
	μ	0.1986	0.0803	[0.0437, 0.3534]	0.14	6.3
	ϕ	0.9290	0.0127	[0.9020, 0.9521]	0.96	25.4
	σ_η^2	0.0580	0.0090	[0.0418, 0.0777]	0.93	38.7

Table 8
Summary statistics of estimated h_t's for $t = 0.2T$ (January 20, 1998) under SV-RV, SV-RVC, SV-SRV, and SV-SRVC models. The last three columns are 2.5th percentile, median, and 97.5th percentile of sampled h_t's.

Model	Data	Mean	Stdev	2.5%	Median	97.5%
SV-RV	RV^1	−0.3647	0.1853	−0.7277	−0.3656	0.0099
	RV^5	−0.3008	0.2342	−0.7647	−0.3009	0.1607
	RV^{10}	−0.1863	0.2556	−0.6914	−0.1844	0.3105
	$TSRV$	−0.4161	0.2714	−0.9524	−0.4135	0.1083
SV-RVC	RV^1	0.8126	0.1557	0.5063	0.8109	1.1153
	RV^5	0.6978	0.2103	0.2874	0.6964	1.1072
	RV^{10}	0.7232	0.2264	0.2851	0.7211	1.1786
	$TSRV$	0.7390	0.2205	0.3044	0.7382	1.1674
SV-SRV	SRV^1	0.8765	0.1506	0.5819	0.8746	1.1702
	SRV^5	0.7120	0.2022	0.3073	0.7130	1.1248
	RV^{10}	0.7058	0.2295	0.2484	0.7032	1.1422
	$TSRV$	0.7199	0.2156	0.3029	0.7169	1.1392
SV-SRVC	SRV^1	0.8127	0.1557	0.5064	0.8111	1.1154
	SRV^5	0.6971	0.2086	0.2870	0.6994	1.1027
	RV^{10}	0.7321	0.2287	0.2856	0.7359	1.1862
	$TSRV$	0.7357	0.2180	0.3091	0.7326	1.1688

Table 9
Estimation results of ASV-RVC model using realized volatilities. The last two columns are p-value of Geweke's convergence diagnostic (CD) test and inefficiency factor, respectively. Priors are set as $c \sim \mathrm{N}(0, 10)$, $\sigma_u^2 \sim \mathrm{IG}(5/2, 0.05/2)$, $(1+\phi)/2 \sim \mathrm{Beta}(20, 1.5)$, and $\Sigma^{-1} \sim W(5, 5\Sigma_0)$, where Σ_0 is constructed from $\sigma_\epsilon = 1$, $\sigma_\eta = 0.1$, and $\rho = -0.3$. See Appendix B for the definition of c and Σ.

		Mean	Stdev	95% interval	CD	Inef.
ASV-RVC	ξ	−1.2408	0.0314	[−1.3033, −1.1793]	0.47	1.6
(RV^1)	σ_u^2	0.0971	0.0044	[0.0887, 0.1057]	0.79	34.9
	μ	0.2116	0.0816	[0.0368, 0.3632]	0.71	263.2
	ϕ	0.9590	0.0079	[0.9429, 0.9738]	0.19	47.9
	σ_η^2	0.0220	0.0030	[0.0167, 0.0282]	0.27	82.4
	ρ	−0.3086	0.0435	[−0.3936, −0.2230]	0.37	25.2
ASV-RVC	ξ	−1.0784	0.0322	[−1.1417, −1.0150]	0.71	4.1
(RV^5)	σ_u^2	0.1553	0.0077	[0.1401, 0.1704]	0.69	23.3
	μ	0.1949	0.0804	[0.0358, 0.3574]	0.15	114.8
	ϕ	0.9390	0.0103	[0.9179, 0.9580]	0.45	23.2
	σ_η^2	0.0465	0.0064	[0.0350, 0.0600]	0.39	46.7
	ρ	−0.2611	0.0405	[−0.3397, −0.1819]	0.30	10.3
ASV-RVC	ξ	−1.0493	0.0325	[−1.1135, −0.9864]	0.32	2.3
(RV^{10})	σ_u^2	0.1959	0.0096	[0.1775, 0.2159]	0.99	30.1
	μ	0.1965	0.0701	[0.0587, 0.3344]	0.89	86.0
	ϕ	0.9292	0.0116	[0.9052, 0.9505]	0.69	34.7
	σ_η^2	0.0543	0.0076	[0.0406, 0.0702]	0.75	58.2
	ρ	−0.2363	0.0411	[−0.3172, −0.1551]	0.85	18.4
ASV-RVC	ξ	−1.4252	0.0317	[−1.4873, −1.3635]	0.25	2.4
($TSRV$)	σ_u^2	0.1783	0.0088	[0.1604, 0.1954]	0.77	32.6
	μ	0.1927	0.0822	[0.0153, 0.3381]	0.67	146.5
	ϕ	0.9364	0.0109	[0.9134, 0.9563]	0.78	42.3
	σ_η^2	0.0497	0.0071	[0.0374, 0.0654]	0.63	57.6
	ρ	−0.2394	0.0420	[−0.3226, −0.1576]	0.50	11.4

Table 10
Estimation results of ASV-SRVC model using scaled realized volatilities. The last two columns are p-value of Geweke's convergence diagnostic (CD) test and inefficiency factor, respectively. Priors are set as $c \sim \mathrm{N}(0, 10)$, $\sigma_u^2 \sim \mathrm{IG}(5/2, 0.05/2)$, $(1+\phi)/2 \sim \mathrm{Beta}(20, 1.5)$, and $\Sigma^{-1} \sim W(5, 5\Sigma_0)$, where Σ_0 is constructed from $\sigma_\epsilon = 1$, $\sigma_\eta = 0.1$, and $\rho = -0.3$. See Appendix B for the definition of c and Σ.

		Mean	Stdev	95% interval	CD	Inef.
ASV-SRVC	ξ	0.0587	0.0314	[−0.0035, 0.1202]	0.11	2.1
(SRV^1)	σ_u^2	0.0977	0.0045	[0.0891, 0.1067]	0.51	38.8
	μ	0.2018	0.0792	[0.0414, 0.3573]	0.35	220.0
	ϕ	0.9600	0.0079	[0.9436, 0.9743]	0.17	40.9
	σ_η^2	0.0215	0.0031	[0.0161, 0.0282]	0.47	81.1
	ρ	−0.3150	0.0440	[−0.4019, −0.2283]	0.12	21.1
ASV-SRVC	ξ	0.0081	0.0320	[−0.0547, 0.0704]	0.15	2.1
(SRV^5)	σ_u^2	0.1553	0.0078	[0.1400, 0.1707]	0.22	28.3
	μ	0.1939	0.0797	[0.0506, 0.3594]	0.75	89.3
	ϕ	0.9390	0.0104	[0.9172, 0.9580]	0.40	31.8
	σ_η^2	0.0465	0.0065	[0.0353, 0.0608]	0.06	50.3
	ρ	−0.2635	0.0407	[−0.3416, −0.1826]	0.45	21.4
ASV-SRVC	ξ	−0.0240	0.0325	[−0.0889, 0.0398]	0.41	2.1
(SRV^{10})	σ_u^2	0.1956	0.0097	[0.1766, 0.2150]	0.86	27.8
	μ	0.1888	0.0773	[0.0402, 0.3474]	0.86	88.1
	ϕ	0.9289	0.0119	[0.9036, 0.9508]	0.89	43.4
	σ_η^2	0.0547	0.0078	[0.0406, 0.0716]	0.54	57.5
	ρ	−0.2378	0.0415	[−0.3187, −0.1574]	0.71	17.1
ASV-SRVC	ξ	−0.0213	0.0318	[−0.0834, 0.0414]	0.38	1.4
($STSRV$)	σ_u^2	0.1789	0.0087	[0.1619, 0.1962]	0.89	21.4
	μ	0.2113	0.0787	[0.0524, 0.3612]	0.75	64.6
	ϕ	0.9371	0.0107	[0.9150, 0.9572]	0.94	28.6
	σ_η^2	0.0488	0.0069	[0.0361, 0.0634]	0.88	41.4
	ρ	−0.2389	0.0410	[−0.3193, −0.1583]	0.80	9.9

Table 11
Log marginal likelihoods for SV-RV and SV-RVC models with different data set. Standard errors are in parentheses.

Data	Model	Likelihood	Prior	Posterior	Log marginal likelihood
RV^1	SV-RV	−5597.33	−6.35	14.29	−5617.97
		(0.47)		(0.06)	(0.47)
	SV-RVC	−4479.01	2.18	17.77	−4494.60
		(0.13)		(0.07)	(0.15)
	ASV-RVC	−3890.44	−0.91	21.96	−3913.31
		(0.10)		(0.06)	(0.11)
RV^5	SV-RV	−5784.13	−10.78	13.23	−5808.14
		(0.38)		(0.08)	(0.39)
	SV-RVC	−5026.91	−4.99	16.30	−5048.20
		(0.11)		(0.09)	(0.14)
	ASV-RVC	−4438.66	−4.66	20.13	−4463.45
		(0.10)		(0.06)	(0.12)
RV^{10}	SV-RV	−5952.94	−9.94	12.91	−5975.78
		(0.31)		(0.04)	(0.31)
	SV-RVC	−5264.31	−6.41	15.83	−5286.55
		(0.19)		(0.08)	(0.20)
	ASV-RVC	−4677.05	−6.26	19.59	−4702.90
		(0.11)		(0.06)	(0.12)
$TSRV$	SV-RV	−6567.04	−10.01	12.62	−6589.67
		(0.44)		(0.04)	(0.44)
	SV-RVC	−5169.68	−5.08	16.19	−5190.95
		(0.15)		(0.06)	(0.17)
	ASV-RVC	−4583.89	−5.60	19.99	−4609.49
		(0.08)		(0.09)	(0.12)

3.3. *Model Comparisons Using Marginal Likelihoods*

For model comparisons, we calculate marginal likelihoods of these models. We follow Chib (1995) and Chib and Jeliazkov (2001) to calculate the posterior ordinate and its numerical standard error. The likelihood ordinate is computed by using the auxiliary particle filter of Pitt and Shephard (1999). We calculate the estimate of the likelihood ordinate and its standard error as the sample mean and standard deviation of the likelihoods from 20 iterations. Tables 11 and 12 show the logarithm of marginal likelihoods (standard errors are in the parentheses).

From these tables, we can confirm that the bias-correction is essential for model fitting. Especially, correcting the bias due to non-trading hours gives more significant improvement (see SV-RV and SV-RVC models) than adjusting it due to the microstructure noise (see SV-SRV and SV-SRVC models). Comparing the log marginal likelihoods of SV-SRV and SV-SRVC models also shows that the benefit for correcting the bias due to microstructure noise disappears. This is probably because 1 minute return, which is the shortest interval return of our data, does not suffer from the noise so much though the bias term is positively estimated in SV-SRVC model. We also observe from these tables that considering asymmetry largely improves the model fitting.

Table 12
Log marginal likelihoods for SV-RV and SV-RVC models with different data set. Standard errors are in parentheses.

Data	Model	Likelihood	Prior	Posterior	Log marginal likelihood
SRV^1	SV-SRV	-4480.92	5.49	15.11	-4490.54
		(0.16)		(0.07)	(0.18)
	SV-SRVC	-4479.16	2.25	17.77	-4494.68
		(0.12)		(0.07)	(0.14)
	ASV-SRVC	-3890.39	-0.83	21.97	-3913.20
		(0.09)		(0.07)	(0.12)
SRV^5	SV-SRV	-5027.22	-2.56	13.72	-5043.50
		(0.14)		(0.06)	(0.15)
	SV-SRVC	-5026.85	-4.56	16.29	-5047.71
		(0.16)		(0.04)	(0.16)
	ASV-SRVC	-4438.68	-4.62	20.19	-4463.49
		(0.14)		(0.06)	(0.15)
SRV^{10}	SV-SRV	-5264.61	-3.90	13.32	-5281.84
		(0.13)		(0.04)	(0.14)
	SV-SRVC	-5264.67	-5.82	15.82	-5286.32
		(0.13)		(0.07)	(0.15)
	ASV-SRVC	-4677.33	-6.22	19.57	-4703.11
		(0.10)		(0.07)	(0.12)
$STSRV$	SV-SRV	-5169.89	-3.06	13.52	-5186.46
		(0.12)		(0.06)	(0.14)
	SV-SRVC	-5169.54	-5.29	16.08	-5190.92
		(0.15)		(0.08)	(0.17)
	ASV-SRVC	-4583.72	-5.55	19.73	-4609.00
		(0.12)		(0.14)	(0.18)

4. Concluding Remarks

In this paper, we proposed modeling daily returns and realized volatility simultaneously extending the well-known stochastic volatility model and described the efficient sampling algorithm for our model to implement Markov chain Monte Carlo simulation. We show that this model can jointly estimate the parameters and the realized volatility bias due to both non-trading hours and the market microstructure noise. Especially, this model allows us to use the realized volatility calculated from all available returns and thus we need not to determine the optimal sampling frequency for calculating the realized volatility. Comparison of marginal likelihood between the simultaneous models using both naive and scaled realized volatilities shows that the effect of non-trading hours is more essential than that of microstructure noise. We also confirm that asymmetry is crucial in stochastic volatility models.

Using Bayesian approach, our model can consider the uncertainty in the estimation of the biases and parameters when we derive the predictive distribution of daily returns, which is important to evaluate the common risk measures such as VaR or expected shortfall. The comparison of the forecasting performances using the risk measures for various models such as the ARFIMA model would be our future work. Further, although we use only the standard normal distribution for daily returns in this paper, our model can be applied to other distributions for daily returns such as Student's t, skewed-t, and normal inverse Gaussian (NIG) distributions. Especially, the NIG distribution has recently attracted the attention of financial economists and econometricians since conditional distribution of the returns is distributed as NIG if the realized volatility is conditionally inverse Gaussian and daily return standardized by the realized volatility is approximately Gaussian (see e.g., Forsberg (2002) and Forsberg and Bollerslev (2002)).

Acknowledgements

The authors thank Herman van Dijk, Gianni Amisano, Philippe Deschamps, Erricos John Kontoghiorghes, and two anonymous referees for their helpful comments. This work is partially supported by Grants-in-Aid for Scientific Research 18330039 and for Special Purposes 18203901 from the Japanese Ministry of Education, Science, Sports, Culture and Technology, and Ishii Memorial Securities Research Promotion Foundation.

Appendix A. Approximation of the conditional posterior density of $\eta^{(j)}$

In the case of $t+k<T$, the log of posterior density (12) is written as

$$\begin{aligned}
&\log f(\eta^{(j)}|h_{t-1},h_{t+k+1},y_t,\ldots,y_{t+k},\theta)\\
&= \text{const.} + \log f(y_{1,t},\ldots,y_{1,t+k}|h_t,\ldots,h_{t+k}) + \log f(y_{2,t},\ldots,y_{2,t+k}|\xi,\sigma_u^2,h_t,\ldots,h_{t+k})\\
&\qquad + \log f(h_{t+k+1}|\mu,\phi,\sigma_\eta^2,h_{t+k}) + \log f(\eta_{t-1},\ldots,\eta_{t+k-1}|\sigma_\eta^2)\\
&= \text{const.} - \sum_{s=t}^{t+k}\left\{\frac{h_s}{2}+\frac{y_{1,s}^2}{2}\exp(-h_s)\right\} - \frac{1}{2\sigma_u^2}\sum_{s=t}^{t+k}(y_{2,s}-\xi-h_s)^2\\
&\qquad - \frac{1}{2\sigma_\eta^2}\{h_{t+k+1}-\mu-\phi(h_{t+k}-\mu)\}^2 - \frac{1}{2\sigma_\eta^2}\sum_{s=t-1}^{t+k-1}\eta_s^2. \qquad \text{(A.1)}
\end{aligned}$$

Following Shephard and Pitt (1997), we approximate this log-posterior density by Taylor expansion of the log of likelihood,

$$l(h_s) \equiv -\frac{h_s}{2} - \frac{y_{1,s}^2}{2}\exp(-h_s),$$

around $h_s=\hat{h}_s$ as follows;

$$
\begin{aligned}
&\log f(\eta^{(j)}|h_{t-1}, h_{t+k+1}, y_t, \ldots, y_{t+k}, \theta) \\
&\approx \text{const.} + \sum_{s=t}^{t+k} \left\{ l(\hat{h}_s) + (h_s - \hat{h}_s) l'(\hat{h}_s) + \frac{1}{2}(h_s - \hat{h}_s)^2 l''(\hat{h}_s) \right\} - \frac{1}{2\sigma_u^2} \sum_{s=t}^{t+k} (y_{2,s} - \xi - h_s)^2 \\
&\quad - \frac{1}{2\sigma_\eta^2} \{h_{t+k+1} - \mu - \phi(h_{t+k} - \mu)\}^2 - \frac{1}{2\sigma_\eta^2} \sum_{s=t-1}^{t+k-1} \eta_s^2 \\
&\equiv \log cg(\eta_{t-1}, \ldots, \eta_{t+k-1}),
\end{aligned}
$$

where

$$
l'(\hat{h}_s) \equiv \frac{\partial l(\hat{h}_s)}{\partial h_s} = \frac{1}{2}\left\{ y_s^2 \exp(-\hat{h}_s) - 1 \right\}, \quad l''(\hat{h}_s) \equiv \frac{\partial^2 l(\hat{h}_s)}{\partial {h_s}^2} = -\frac{y_s^2}{2} \exp(-\hat{h}_s).
$$

On the other hand, when sampling the last block, i.e. $t + k = T$, the log of posterior density is written as, excluding h_{t+k+1} in the condition,

$$
\begin{aligned}
&\log f(\eta^{(j)}|h_{t-1}, y_t, \ldots, y_{t+k}, \theta) \\
&= \text{const.} - \sum_{s=t}^{t+k} \left\{ \frac{h_s}{2} + \frac{y_{1,s}^2}{2} \exp(-h_s) \right\} - \frac{1}{2\sigma_u^2} \sum_{s=t}^{t+k} (y_{2,s} - \xi - h_s)^2 - \frac{1}{2\sigma_\eta^2} \sum_{s=t-1}^{t+k-1} \eta_s^2.
\end{aligned}
$$

Similar to the case of $t + k < T$, we approximate this log-density as

$$
\begin{aligned}
&\log f(\eta^{(j)}|h_{t-1}, y_t, \ldots, y_{t+k}, \theta) \\
&\approx \text{const.} + \sum_{s=t}^{t+k} \left\{ l(\hat{h}_s) + (h_s - \hat{h}_s) l'(\hat{h}_s) + \frac{1}{2}(h_s - \hat{h}_s)^2 l''(\hat{h}_s) \right\} - \frac{1}{2\sigma_u^2} \sum_{s=t}^{t+k} (y_{2,s} - \xi - h_s)^2 - \frac{1}{2\sigma_\eta^2} \sum_{s=t-1}^{t+k-1} \eta_s^2 \\
&\equiv \log cg(\eta_{t-1}, \ldots, \eta_{t+k-1}).
\end{aligned}
$$

Then we can consider $g(\eta_{t-1}, \ldots, \eta_{t+k-1})$ as the conditional density of linear Gaussian state space model,

$$
\begin{aligned}
\hat{y}_{1,s} &= h_s + \hat{\epsilon}_s, \quad \hat{\epsilon}_s \sim \mathrm{N}(0, v_s), \\
y_{2,s} &= \xi + h_s + u_s, \quad u_s \sim \mathrm{N}(0, \sigma_u^2),
\end{aligned}
$$

and

$$
h_{s+1} = \mu + \phi(h_s - \mu) + \eta_s, \quad \eta_s \sim \mathrm{N}(0, \sigma_\eta^2),
$$

where $\hat{y}_{1,s}$ and v_s are defined as,

(i) if $s = t, t+1, \ldots, t+k-1$ or $s = t + k = T$,

$$
\hat{y}_{1,s} = \hat{h}_s + v_s l'(\hat{h}_s), \quad v_s = -\frac{1}{l''(\hat{h}_s)},
$$

(ii) if $s = t + k < T$,

$$
\hat{y}_s = \hat{h}_s + v_s \left[l'(\hat{h}_s) + \frac{\phi}{\sigma_\eta^2} \left\{ h_{t+k+1} - \mu - \phi(\hat{h}_s - \mu) \right\} \right], \quad v_s = \frac{\sigma_\eta^2}{\phi^2 - \sigma_\eta^2 l''(\hat{h}_s)}.
$$

The correction in (ii) is necessary except the last block ($s = t + k = T$) because of the existence of the fourth term in (A.1) (see Watanabe and Omori (2004)).

Appendix B. Estimation of ASV-RVC Model

We first rewrite ASV-RVC model in (8) and (9) as

$$
\begin{aligned}
y_{1,t} &= \sigma_\epsilon \exp(\alpha_t/2)\epsilon_t, \\
y_{2,t} &= c + \alpha_t + \sigma_u u_t, \\
\alpha_{t+1} &= \phi\alpha_t + \sigma_\eta \eta_t, \\
\alpha_1 &\sim \mathrm{N}(0, \sigma_\eta^2/(1 - \phi^2)),
\end{aligned}
$$

and

$$\begin{pmatrix} \epsilon_t \\ u_t \\ \eta_t \end{pmatrix} \sim \mathrm{N}\left(\begin{pmatrix} 0 \\ 0 \\ 0 \end{pmatrix}, \begin{pmatrix} 1 & 0 & \rho \\ 0 & 1 & 0 \\ \rho & 0 & 1 \end{pmatrix}\right).$$

New parameters are defined by parameters in (8) and (9) as $\sigma_\epsilon = \exp(\mu/2)$, $\alpha_t = h_t - \mu$, and $c = \xi + \mu$. Similar to symmetric models, efficient sampling α_t is the key to estimate the asymmetric model. Therefore, we first describe the sampling algorithm for α_t.

B.1. *Efficient Sampler for the Latent Volatilities with Asymmetry*

To make the sampling efficient, we use the block sampler by Omori and Watanabe (2008). As in Section 2.3.1, we first divide $(\alpha_1, \ldots, \alpha_T)$ into $K+1$ blocks, $(\alpha_{k_{j-1}+1}, \ldots, \alpha_{k_j})'$ for $j = 1, \ldots, K+1$, with $k_0 = 0$ and $k_{K+1} = T$, where $k_j - k_{j-1} \geq 2$. We select K knots, $(k_1, \ldots, k_K)$, randomly (see Section 2.3.1 for the detail) and sample the error term $(\eta_{k_{j-1}}, \ldots, \eta_{k_{j-1}})$ instead of $(\alpha_{k_{j-1}+1}, \ldots, \alpha_{k_j})$ simultaneously from their full conditional distribution.

Suppose that $k_{j-1} = s$ and $k_j = s + m$ for the jth block and let y_t denote $y_t = (y_{1,t}, y_{2,t})$. Then $(\eta_s, \ldots, \eta_{s+m-1})$ are sampled simultaneously from the following full conditional distribution:

$$f(\eta_s, \ldots, \eta_{s+m-1} | \alpha_s, \alpha_{s+m+1}, y_s, \ldots, y_{s+m}) \propto \prod_{t=s}^{s+m} f(y_t | \alpha_t, \alpha_{t+1}) \prod_{t=s}^{s+m-1} f(\eta_t), \tag{B.1}$$

for $s + m < T$, and

$$f(\eta_s, \ldots, \eta_{s+m-1} | \alpha_s, y_s, \ldots, y_{s+m}) \propto \prod_{t=s}^{s+m-1} f(y_t | \alpha_t, \alpha_{t+1}) f(y_T | \alpha_T) \prod_{t=s}^{s+m-1} f(\eta_t), \tag{B.2}$$

for $s + m = T$. The logarithm of $f(y_t|\alpha_t, \alpha_{t+1})$ or $f(y_T|\alpha_T)$ in (B.1) and (B.2) (excluding constant term) is given by

$$l_t = -\frac{\alpha_t}{2} - \frac{(y_{1,t} - \mu_t)^2}{2\sigma_t^2} - \frac{(y_{2,t} - c - \alpha_t)^2}{2\sigma_u^2},$$

where

$$\mu_t = \begin{cases} \rho \sigma_\epsilon \sigma_\eta^{-1} (\alpha_{t+1} - \alpha_t) \exp(\alpha_t/2), & t < T, \\ 0, & t = T, \end{cases}$$

and

$$\sigma_t^2 = \begin{cases} (1 - \rho^2) \sigma_\epsilon^2 \exp(\alpha_t), & t < T, \\ \sigma_\epsilon^2 \exp(\alpha_T), & t = T. \end{cases}$$

Then the logarithm of (B.1) and (B.2) is $-\sum_{t=s}^{s+m-1} \eta^2/2 + L$ (excluding a constant term) where

$$L = \begin{cases} \displaystyle\sum_{t=s}^{s+m} l_s - \frac{(\alpha_{s+m+1} - \phi \alpha_{s+m})^2}{2\sigma_\eta^2}, & s + m < T, \\ \displaystyle\sum_{t=s}^{s+m} l_s, & s + m = T. \end{cases}$$

Further define

$$d = (d_{s+1}, \ldots, d_{s+m})', \quad d_t = \frac{\partial L}{\partial \alpha_t}, \quad t = s+1, \ldots, s+m,$$

$$Q = -E\left(\frac{\partial^2 L}{\partial \alpha \partial \alpha'}\right) = \begin{pmatrix} A_{s+1} & B_{s+2} & 0 & \cdots & 0 \\ B_{s+2} & A_{s+2} & B_{s+3} & \cdots & 0 \\ 0 & B_{s+3} & A_{s+3} & \ddots & \vdots \\ \vdots & \ddots & \ddots & \ddots & B_{s+m} \\ 0 & \cdots & 0 & B_{s+m} & A_{s+m} \end{pmatrix},$$

$$A_t = -E\left(\frac{\partial^2 L}{\partial \alpha_t^2}\right), \quad t = s+1, \ldots, s+m, \tag{B.3}$$

and

$$B_t = -E\left(\frac{\partial^2 L}{\partial \alpha_t \partial \alpha_{t-1}}\right), \quad t = s+2, \ldots, s+m, \quad B_{s+1} = 0, \tag{B.4}$$

where $s \geq 0$ ($t \geq 1$ for (B.3) and $t \geq 2$ for (B.4)) and $\alpha = (\alpha_{s+1}, \ldots, \alpha_{s+m})'$. The first derivative of L with respect to α_t is given by

$$d_t = -\frac{1}{2} + \frac{(y_t - \mu_t)^2}{2\sigma_t^2} + \frac{y_t - \mu_t}{\sigma_t^2}\frac{\partial \mu_t}{\partial \alpha_t} + \frac{y_{t-1} - \mu_{t-1}}{\sigma_{t-1}^2}\frac{\partial \mu_{t-1}}{\partial \alpha_t} + \frac{y_{2,t} - c - \alpha_t}{\sigma_u^2},$$

for $t = s+1, \ldots, s+m-1$ or $t = s+m = T$, and

$$d_t = -\frac{1}{2} + \frac{(y_t - \mu_t)^2}{2\sigma_t^2} + \frac{y_t - \mu_t}{\sigma_t^2}\frac{\partial \mu_t}{\partial \alpha_t} + \frac{y_{t-1} - \mu_{t-1}}{\sigma_{t-1}^2}\frac{\partial \mu_{t-1}}{\partial \alpha_t} + \frac{\phi(\alpha_{t+1} - \phi\alpha_t)}{\sigma_\eta^2} + \frac{y_{2,t} - c - \alpha_t}{\sigma_u^2},$$

for $t = s+m < T$, where

$$\frac{\partial \mu_t}{\partial \alpha_t} = \begin{cases} \rho\sigma_\epsilon\sigma_\eta^{-1}\{-\phi + (\alpha_{t+1} - \phi\alpha_t)/2\}\exp(\alpha_t/2), & t = 1, \ldots, T-1, \\ 0, & t = T, \end{cases}$$

and

$$\frac{\partial \mu_{t-1}}{\partial \alpha_t} = \begin{cases} 0, & t = 1, \\ \rho\sigma_\epsilon\sigma_\eta^{-1}\exp(\alpha_{t-1}/2), & t = 2, \ldots, T. \end{cases}$$

Taking expectations of second derivatives multiplied by -1 with respect to y_t's, we obtain the A_t's and B_t's as follows:

$$A_t = \begin{cases} \frac{1}{2} + \sigma_t^{-2}\left(\frac{\partial \mu_t}{\partial \alpha_t}\right)^2 + \sigma_{t-1}^{-2}\left(\frac{\partial \mu_{t-1}}{\partial \alpha_t}\right)^2 + \sigma_u^{-2}, & t = s+1, \ldots, s+m-1 \text{ or } t = s+m = T, \\ \frac{1}{2} + \sigma_t^{-2}\left(\frac{\partial \mu_t}{\partial \alpha_t}\right)^2 + \sigma_{t-1}^{-2}\left(\frac{\partial \mu_{t-1}}{\partial \alpha_t}\right)^2 + \phi^2\sigma_\eta^{-2} + \sigma_u^{-2}, & t = s+m < T, \end{cases}$$

and

$$B_t = \sigma_{t-1}^{-2}\frac{\partial \mu_{t-1}}{\partial \alpha_{t-1}}\frac{\partial \mu_{t-1}}{\partial \alpha_t}, \quad t = 2, \ldots, T.$$

Applying the second order Taylor expansion to (B.1) will produce the approximating normal density $f^*(\eta_s, \ldots, \eta_{s+m-1}|\alpha_s, \alpha_{s+m+1}, y_s, \ldots, y_{s+m})$ as follows (see Omori and Watanabe (2008) for details):

$$\log f(\eta_s,\ldots,\eta_{s+m-1}|\alpha_s,\alpha_{s+m+1},y_s,\ldots,y_{s+m})$$
$$\approx \text{const} - \frac{1}{2}\sum_{t=s}^{s+m-1}\eta_t^2 + \hat{L} + \left.\frac{\partial L}{\partial \eta'}\right|_{\eta=\eta'}(\eta-\hat{\eta}) + \frac{1}{2}(\eta-\hat{\eta})'\, E\left(\frac{\partial^2 L}{\partial\eta\partial\eta'}\right)\Bigg|_{\eta=\hat{\eta}}(\eta-\hat{\eta})$$
$$= \text{const} - \frac{1}{2}\sum_{t=s}^{s+m-1}\eta_t^2 + \hat{L} + \hat{d}'(\alpha-\hat{\alpha}) - \frac{1}{2}(\alpha-\hat{\alpha})'\hat{Q}(\alpha-\hat{\alpha})$$
$$= \text{const} + \log f^*(\eta_s,\ldots,\eta_{s+m-1}|\alpha_s,\alpha_{s+m+1},y_s,\ldots,y_{s+m}),$$

where $\hat{d}$, $\hat{L}$, and $\hat{Q}$ denote d, L, and Q evaluated at $\alpha=\hat{\alpha}$ (or, equivalently, at $\eta=\hat{\eta}$). The expectations are taken with respect to y_t's conditional on α_t's. Similarly, we can obtain the normal density which approximates (B.2).

To make the linear Gaussian state-space model corresponding to the approximating density, we first compute the following D_t, K_t, J_t, and b_t for $t=s+2,\ldots,s+m$ recursively,

$$D_t = \hat{A}_t - D_{t-1}^{-1}\hat{B}_t^2, \quad D_{s+1}=\hat{A}_{s+1},$$
$$K_t = \sqrt{D_t},$$
$$J_t = \hat{B}_t K_{t-1}^{-1}, \quad J_{s+1}=0, \quad J_{s+m+1}=0,$$

and

$$b_t = \hat{d}_t - J_t K_{t-1}^{-1} b_{t-1}, \quad b_{s+1}=\hat{d}_{s+1}.$$

Second, we define auxiliary variables $\hat{y}_t = \hat{\gamma}_t + D_t^{-1}b_t$ where

$$\hat{\gamma}_t = \hat{\alpha}_t + K_t^{-1}J_{t+1}\hat{\alpha}_{t+1}, \quad t=s+1,\ldots,s+m.$$

Then the approximating density corresponds to the density of the linear Gaussian state-space model given by

$$\hat{y}_t = Z_t\alpha_t + G_t\zeta_t, \quad t=s+1,\ldots,s+m,$$

and

$$\alpha_{t+1} = \phi\alpha_t + H_t\zeta_t, \quad t=s,s+1,\ldots,s+m, \quad \zeta_t\sim \mathrm{N}(0,I),$$

where

$$Z_t = 1 + K_t^{-1}J_{t+1}\phi, \quad G_t = K_t^{-1}(\,1,\ J_{t+1}\sigma_\eta\,), \quad H_t = (\,0,\ \sigma_\eta\,).$$

As in Section 2.3.1, we can sample $(\eta_s,\ldots,\eta_{s+m-1})$ from the full posterior distribution in (B.1) and (B.2) by applying the simulation smoother to this state-space model and using ARMH algorithm. Similarly, the mode of η_t's (or equivalently α_t's) is obtained by applying Kalman filter and the disturbance smoother to the state-space model repeatedly.

B.2. *Sampling Parameters*

Let Y, y_t, Σ, and θ denote $Y=(y_1,\ldots,y_T)$, $y_t=(y_{1,t},y_{2,t})$,

$$\Sigma = \begin{pmatrix} \sigma_\epsilon^2 & \rho\sigma_\epsilon\sigma_\eta \\ \rho\sigma_\epsilon\sigma_\eta & \sigma_\eta^2 \end{pmatrix},$$

and $\theta=(\phi,\Sigma,\sigma_u^2,c)$, respectively. Further, we write all parameters of θ except x as θ_{-x}. We first initialize $\{\alpha_t\}_{t=1}^T$ and θ and proceed an MCMC implementation in 5 steps.

1. Sample $\{\alpha_t\}_{t=1}^T|\theta,Y$.
   (a) Generate K stochastic knots $(k_1,\ldots,k_K)$ and set $k_0=0$, $k_{K+1}=T$.
   (b) Sample $\{\alpha_t\}_{t=k_{i-1}+1}^{k_i}|\{\alpha_t|t\le k_{i-1}, t>k_i\},\theta,Y$ for $i=1,\ldots,K+1$.

2. Sample $\phi|\{\alpha_t\}_{t=1}^T, \theta_{-\phi}, Y$.
3. Sample $\Sigma|\{\alpha_t\}_{t=1}^T, \theta_{-\Sigma}, Y$.
4. Sample $\sigma_u^2|\{\alpha_t\}_{t=1}^T, \theta_{-\sigma_u^2}, Y$.
5. Sample $c|\{\alpha_t\}_{t=1}^T, \theta_{-c}, Y$.

In the first step, we sample $\{\alpha_t\}_{t=1}^T$ by applying block the sampler to each block as in the previous subsection.

In the second step, let $\pi(\phi)$ denote a prior probability density for ϕ. The logarithm of the conditional posterior density for ϕ (excluding a constant term) is given by

$$\log \pi(\phi) + \frac{1}{2}\log(1-\phi^2) - \frac{\alpha_1^2(1-\phi^2)}{2\sigma_\eta^2} - \frac{\sum_{t=1}^{T-1}\{\alpha_{t+1} - \phi\alpha_t - \rho\sigma_\eta\sigma_\epsilon^{-1}\exp(-\alpha_t/2)y_{1,t}\}^2}{2(1-\rho^2)\sigma_\eta^2}.$$

We propose a candidate for the MH algorithm using a truncated normal distribution on $(-1, 1)$, with mean μ_ϕ and variance σ_ϕ^2 (which we denote by $\phi \sim TN_{(-1,1)}(\mu_\phi, \sigma_\phi^2)$) where

$$\mu_\phi = \frac{\sum_{t=1}^{T-1}\alpha_t(\alpha_{t+1} - \rho\sigma_\eta\sigma_\epsilon^{-1}\exp(-\alpha_t/2)y_{1,t})}{\rho^2\alpha_1^2 + \sum_{t=2}^{T-1}\alpha_t^2}, \quad \sigma_\phi^2 = \frac{(1-\rho^2)\sigma_\eta^2}{\rho^2\alpha_1^2 + \sum_{t=2}^{T-1}\alpha_t^2}.$$

Given the current sample ϕ_x, generate $\phi_y \sim TN_{(-1,1)}(\mu_\phi, \sigma_\phi^2)$ and accept it with probability

$$\min\left\{\frac{\pi(\phi_y)\sqrt{1-\phi_y^2}}{\pi(\phi_x)\sqrt{1-\phi_x^2}},\ 1\right\}.$$

In the third step, we assume that a prior distribution of Σ^{-1} follows Wishart distribution (which we denote by $\Sigma^{-1} \sim W(\nu_0, \Sigma_0)$). Then the logarithm of the conditional posterior density of Σ (excluding a constant term) is

$$-\log\sigma_\eta - \frac{\alpha_1^2(1-\phi^2)}{2\sigma_\eta^2} - \frac{\nu_1+3}{2}\log|\Sigma| - \frac{1}{2}\mathrm{tr}(\Sigma_1^{-1}\Sigma^{-1}) - \log\sigma_\epsilon - \frac{y_{1,T}^2}{2\sigma_\epsilon^2\exp(\alpha_T)}$$

where

$$\nu_1 = \nu_0 + T - 1, \quad \Sigma_1^{-1} = \Sigma_0^{-1} + \sum_{t=1}^{T-1} x_t x_t', \quad x_t = (y_t\exp(-\alpha_t/2),\ \alpha_{t+1} - \phi\alpha_t)'.$$

We sample Σ using MH algorithm with a proposal $\Sigma^{-1} \sim W(\nu_1, \Sigma_1)$. Given the current value Σ_x^{-1}, generate $\Sigma_y^{-1} \sim W(\nu_1, \Sigma_1)$ and accept it with probability

$$\min\left\{\frac{\sigma_{\eta,y}^{-1}\sigma_{\epsilon,y}^{-1}\exp\left(-\frac{\alpha_1^2(1-\phi^2)}{2\sigma_{\eta,y}^2} - \frac{y_{1,T}^2}{2\sigma_{\epsilon,y}^2\exp(\alpha_T)}\right)}{\sigma_{\eta,x}^{-1}\sigma_{\epsilon,x}^{-1}\exp\left(-\frac{\alpha_1^2(1-\phi^2)}{2\sigma_{\eta,x}^2} - \frac{y_{1,T}^2}{2\sigma_{\epsilon,x}^2\exp(\alpha_T)}\right)}, 1\right\}.$$

In the last two steps, we use similar priors as in Section 2.3.2. Since c and σ_u^2 only depend on $y_{2,t}$'s given α_t's, we can sample these parameters in a similar way.

References

Aït-Sahalia, Y., Mancini, L., 2007. Out of sample forecasts of quadratic variation, forthcoming in Journal of Econometrics.

Aït-Sahalia, Y., Mykland, P. A., Zhang, L., 2006. Ultra high frequency volatility estimation with dependent microstructure noise, mimeo (w11380, NBER).

Andersen, T. G., Bollerslev, T., 1998. Answering the skeptics: Yes, standard volatility models do provide accurate forecasts. International Economic Review 39, 885–905.

Andersen, T. G., Bollerslev, T., Diebold, F. X., Ebens, H., 2001a. The distribution of realized stock return volatility. Journal of Financial Economics 61, 43–76.

Andersen, T. G., Bollerslev, T., Diebold, F. X., Labys, P., 2001b. The distribution of realized exchange rate volatility. Journal of the American Statistical Association 96, 42–55.

Bandi, F. M., Russell, J. R., 2005. Microstructure noise, realized volatility, and optimal sampling, mimeo. (Graduate School of Business, University of Chicago).

Barndorff-Nielsen, O. E., Shephard, N., 2001. Non-Gaussian Ornstein-Uhlenbeck-based models and some of their uses in financial economics. Journal of the Royal Statistical Society B 63, 167–241.

Black, F., 1976. Studies of stock market volatility changes. In: 1976 Proceedings of the American Statistical Association, Business and Economic Statistics Section, pp. 177-181.

Chib, S., 1995. Marginal likelihood from the Gibbs output. Journal of the American Statistical Association 90, 1313–1321.

Chib, S., 2001. Markov chain Monte Carlo methods: Computation and inference. In: Heckman, J. J., Leamer, E. (Eds.), Handbook of Econometrics. Vol. 5. North-Holland, Amsterdam, pp. 3569–3649.

Chib, S., Greenberg, E., 1995. Understanding the Metropolis-Hastings algorithm. American Statistician 49, 327–335.

Chib, S., Jeliazkov, I., 2001. Marginal likelihood from the Metropolis-Hastings output. Journal of the American Statistical Association 96, 270–281.

Christie, A. A., 1982. The stochastic behavior of common stock variances-value, leverage and interest rate effects. Journal of Financial Economics 10, 407–432.

de Jong, P., Shephard, N., 1995. The simulation smoother for time series models. Biometrika 82, 339–350.

Diebold, F. X., 1988. Empirical Modeling of Exchange Rate Dynamics. Springer-Verlag, New York.

Doornik, J. A., 2002. Object-Oriented Matrix Programming Using Ox, 3rd ed. Timberlake Consultants Press and Oxford, London.

Durbin, J., Koopman, S. J., 2002. A simple and efficient simulation smoother for state space time series analysis. Biometrika 89, 603–616.

Fama, E. F., 1965. The behavior of stock-market prices. The Journal of Business 38, 34–105.

Forsberg, L., 2002. On the normal inverse Gaussian distribution in modeling volatility in the financial markets, doctoral thesis, Studia Statistica Upsaliensia 5, Christofferson A, Jöreskog KG (eds). Uppsala University Library.

Forsberg, L., Bollerslev, T., 2002. Bridging the gap between the distribution of realized (ECU) volatility and ARCH modelling (of the EURO): The GARCH-NIG model. Journal of Applied Econometrics 17, 535–548.

French, K. R., Roll, R., 1986. Stock return variances: The arrival of information and the reaction of traders. Journal of Financial Economics 17, 5–26.

Geweke, J., 1992. Evaluating the accuracy of sampling-based approaches to the calculation of posterior moments. In: Bernardo, J. M., Berger, J. O., Dawid, A. P., Smith, A. F. M. (Eds.), Bayesian Statistics. Vol. 4. Oxford University Press, New York, pp. 169–193.

Ghysels, E., Harvey, A. C., Renault, E., 1996. Stochastic volatility. In: Maddala, G. S., Rao, C. R. (Eds.), Handbook of Statistics. North-Holland, Amsterdam, pp. 119–191.

Hansen, P. R., Lunde, A., 2005. A forecast comparison of volatility models: Does anything beat a GARCH(1,1)? Journal of Applied Econometrics 20, 873–889.

Hansen, P. R., Lunde, A., 2006. Realized variance and market microstructure noise. Journal of Business & Economic Statistics 24, 127–161.

Hasbrouck, J., 2007. Empirical Market Microstructure: The Institutions, Economics And Econometrics of Securities Trading. Oxford University Press, New York.

Jacquier, E., Polson, N. G., Rossi, P. E., 1994. Bayesian analysis of stochastic volatility models (with discussion). Journal of Business & Economic Statistics 12, 371–417.

Kim, S., Shephard, N., Chib, S., 1998. Stochastic volatility: Likelihood inference and comparison with ARCH models. Review of Economic Studies 65, 361–393.

Koopman, S. J., 1993. Disturbance smoother for state space models. Biometrika 80, 117–126.

Martens, M., 2002. Measuring and forecasting S&P 500 index-futures volatility using high-frequency data. The Journal of Futures Markets 22, 497–518.

McAleer, M., Medeiros, M. C., 2006. Realized volatility: A review, forthcoming in Econometric Reviews.

Nelson, D. B., 1991. Conditional heteroskedasticity in asset returns: A new approach. Econometrica 59, 347–370.

O'Hara, M., 1995. Market Microstructure Theory. Blackwell, Oxford.

Omori, Y., Watanabe, T., 2008. Block sampler and posterior model estimation for asymmetric stochastic volatility models. Computational Statistics & Data Analysis 52, 2892–2910.

Pitt, M. K., Shephard, N., 1999. Filtering via simulation: Auxiliary particle filters. Journal of the American Statistical Association 94, 590–599.

Shephard, N., 1996. Statistical aspects of ARCH and stochastic volatility. In: Cox, D. R., Hinkley, D. V., Barndorff-Nielsen, O. E. (Eds.), Time Series Models in Econometrics, Finance and Other Fields. Chapman & Hall, New York, pp. 1–67.

Shephard, N., Pitt, M. K., 1997. Likelihood analysis of non-Gaussian measurement time series. Biometrika 84, 653–667.

Taylor, S. J., 1986. Modeling Financial Time Series. John Wiley & Sons.

Tierney, L., 1994. Markov chains for exploring posterior distributions (with discussion). American Statistician 21, 1701–1762.

Watanabe, T., 2007. Realized volatility–A survey with the application to the Japanese stock market (in Japanese). Economic Review 58, 352–373.

Watanabe, T., Omori, Y., 2004. A multi-move sampler for estimating non-Gaussian time series models: Comments on Shephard

& Pitt (1997). Biometrika 91, 246–248.

Zhang, L., 2006. Efficient estimation of stochastic volatility using noisy observations: A multi-scale approach. Bernoulli 12, 1019–1043.

Zhang, L., Mykland, P. A., Aït-Sahalia, Y., 2005. A tale of two time scales: Determining integrated volatility with noisy high frequency data. Journal of the American Statistical Association 100, 1394–1411.